CMD Workshop 36 : Spintronics course
in Center for Spintronics Research Network (CSRN),
Graduate School of Engineering Science, Osaka University.

February 18, 2020

Spintronic Interface design
(スピントロニクス・インターフェース・デザイン)

Yoshio Miura

National Institute for Materials Science (NIMS)

Research Center for Magnetic and Spintronic Materials (CMSM)

Spin Theory Group

Topics

0. Introduction on spintronics

1. First-Principles Study on magneto-crystalline anisotropy of Fe/MgO(001) and Fe/$MgAl_2O_4$(001)

K. Masuda and Y. Miura, PRB **98**, 224421 (2018).

2. First-Principles Study on magnetic damping of Fe/MgO(001)

Y. Miura, in preparation

3. First-Principles Study on magneto Seebeck Effect in magnetic tunnel junctions

K. Yamamoto, K. Masuda, K. Uchida, Y. Miura arXiv:1912.01207

Instroduction

Magnetic tunnel junction (MTJs)

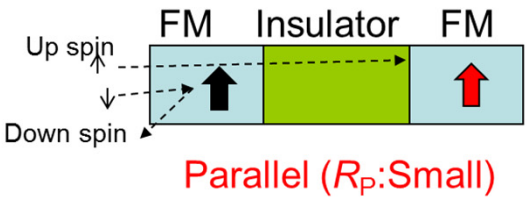

Parallel (R_P:Small)

(FM: Ferromagnetic metal)

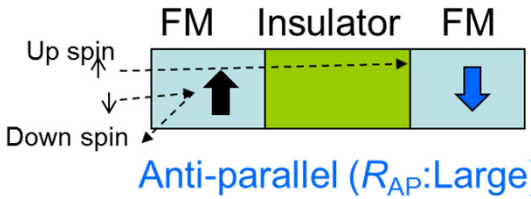

Anti-parallel (R_{AP}:Large)

Tunneling magnetoresistance (TMR)

$$\text{TMR ratio} = \frac{R_{AP} - R_P}{R_{AP}}$$

Magnetoresistive Random Access Memory (MRAM)

- Non volatile memory
- Fast writing speed (10～50ns)
- Low electricity consumption (～30μW)
- Long endurance (10 years)

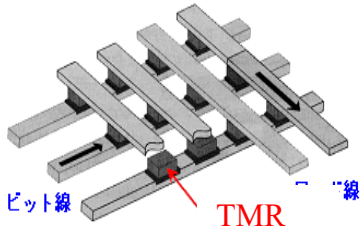

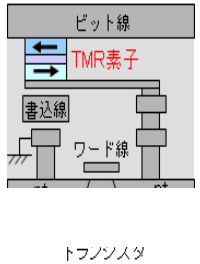

Everspin
64Mbit MRAM

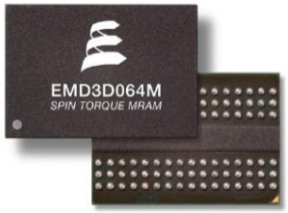

Magnetic censer

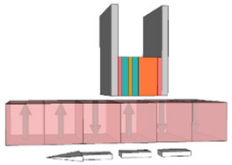

HDD read-out-head

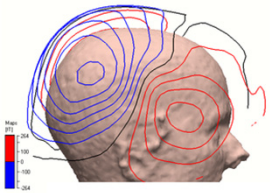

Earth's magnetic field censer・current censer for car・biomagnetic censer

Corresponding to SQUID

Magnetization reversal in MTJs

1. Magnetic field by current

problem : ・complicate circuit.
・current∝1/device-size

Effects of demagnetizing field increase the critical current for writing with decreasing size of device

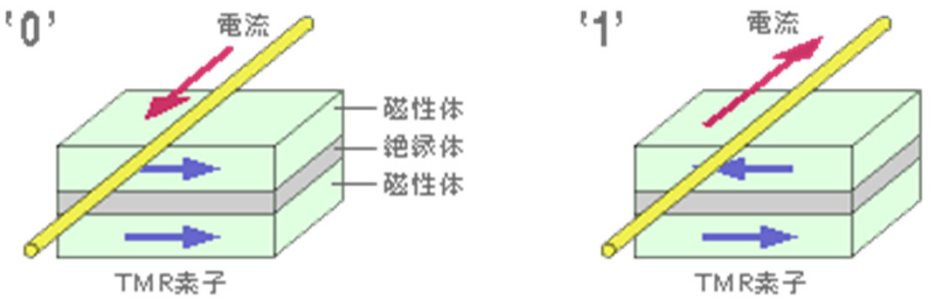

2. Spin transfer torque（STT）

The spin flip of conductive electron give the torque to the local spin moment due to the angular momentum conservation

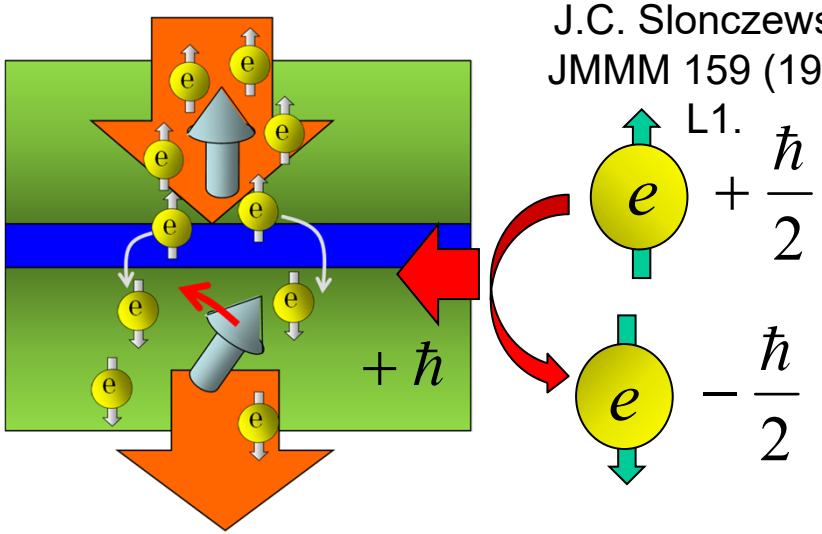

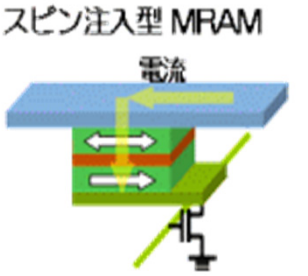

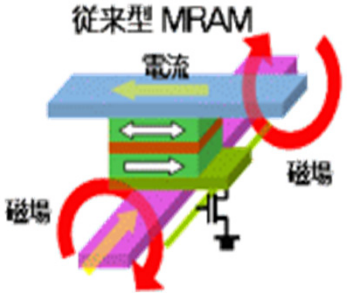

・simple circuit
・current∝device-size

Tohoku Univ. Ando lab. HP

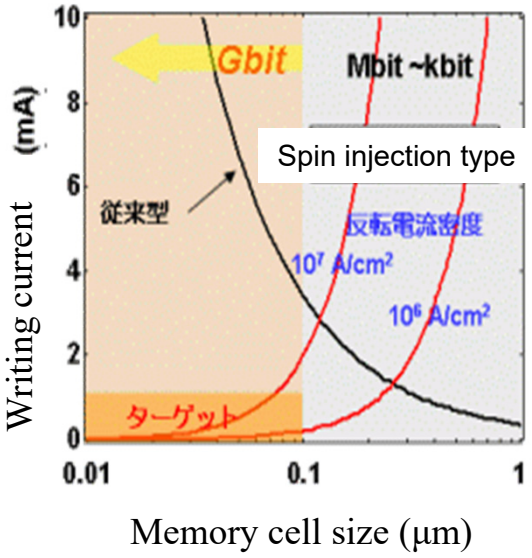

Magnetization reversal by spin transfer torque (STT)

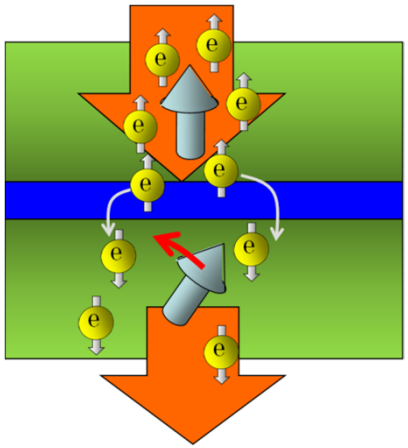

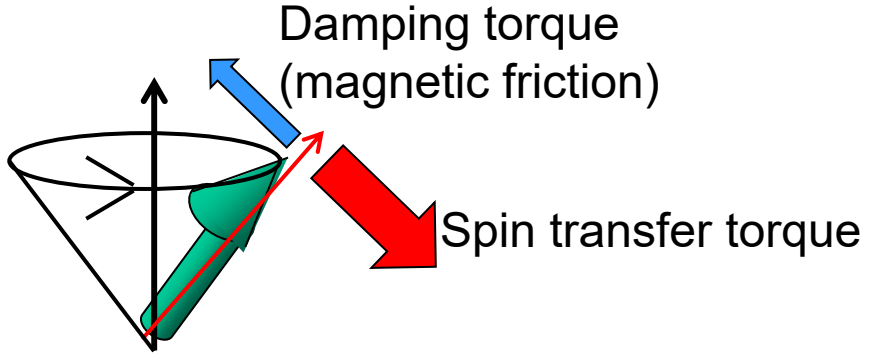

Reduction of critical current density (J_{c0})

$(10^7 \mathrm{A/cm^2} \Rightarrow 10^5 \mathrm{A/cm^2})$

$$J_{c0} \propto \alpha M_S [H_{\mathrm{anti}} \pm 4\pi M_S]\ t/P$$

J.C. Slonczewski, JMMM 159 (1996) L1.

α : Magnetic damping constant
M_S : Saturation Magnetization
$H_{\mathrm{anti}} \pm 4\pi M_S$: Effective anisotropy field
P : Spin polarization
t : Thickness of FM layer

1. High spin polarization (P)

2. Low damping constant(α)

3. Perpendicular magnetic anisotropy(PMA) H_{anti}-$4\pi M_s$

Topics

0. Introduction on spintronics

1. First-Principles Study on magneto-crystalline anisotropy of Fe/MgO(001) and Fe/$MgAl_2O_4$(001)

K. Masuda and Y. Miura, PRB **98**, 224421 (2018).

2. First-Principles Study on magnetic damping of Fe/MgO(001)

Y. Miura, in preparation

3. First-Principles Study on magneto Seebeck Effect in magnetic tunnel junctions

K. Yamamoto, K. Masuda, K. Uchida, Y. Miura arXiv:1912.01207

Thermal stability of magnetization in MTJs

To achieve ultra high density MRAM

In-plane MTJ

Side view

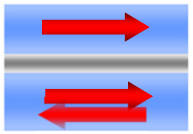

Top view

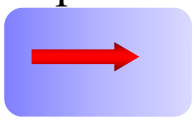

Aspect ratio >2

Perpendicular MTJ

Side view

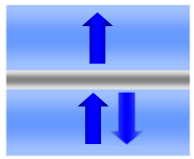

Top view

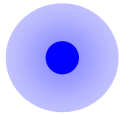

For 10 year's write endurance

Thermal stability factor $\frac{K_u V}{k_B T} \geq 60$

K_u : uniaxial magnetic anisotropy

Large K_u is required with decreasing volume towards scaling down of device dimensions

Examples of Perpendicular MTJ

Using $L1_0$-type FePt, CoPt, CoFePd alloys and its multilayered structures

[1] M. Yoshikawa, *et al.*, IEEE Trans. Magn. vol.**44** 2573 (2008). (Toshiba)

[2] K. Yakushiji, *et al.*, APEX vol. **3** 053003 (2010). (AIST)

[3] K. Mizunuma *et al.*, APEX vol. **4** 023002 (2011). (Tohoku)

Interfacial Perpendicular Magnetic Anisotropy (PMA) for MgO

S. Ikeda, *et al*., Nature Materials **9**, 721 (2010).

- CoFeB/MgO/CoFeB(001)

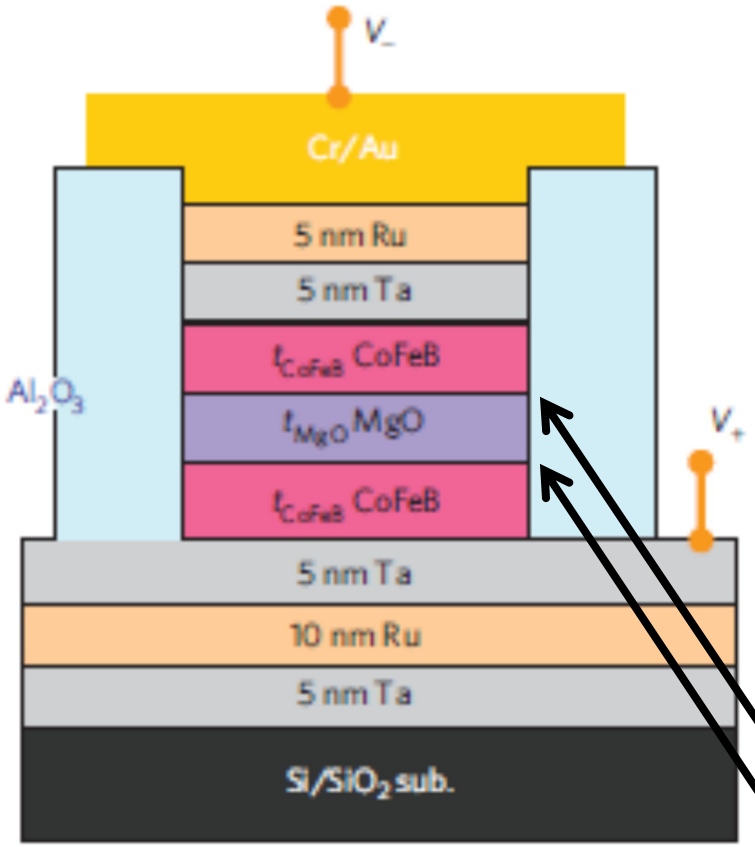

TMR ratio of 120% at 300K

In-plane magnetization (t_{CoFeB}=2.0nm)

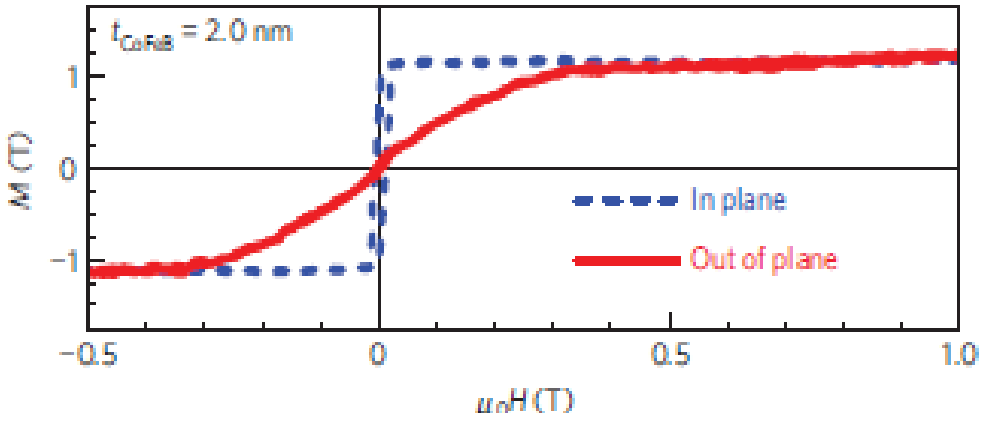

Perpendicular magnetization (t_{CoFeB}<1.3nm)

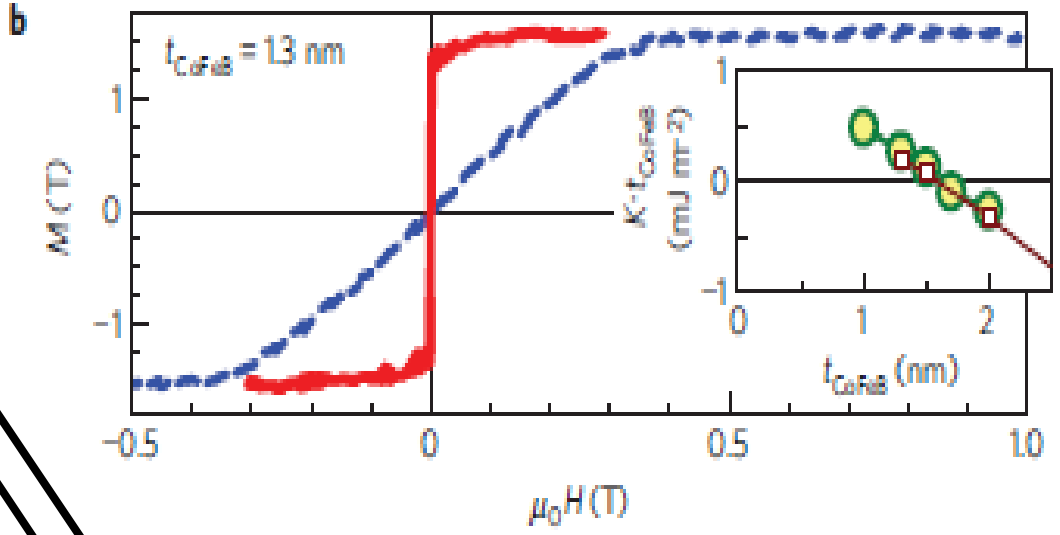

Interfacial perpendicular MCA of Fe/MgO(001), which is K_i=1.30 mJ/m^2

Interfacial Perpendicular Magnetic Anisotropy(PMA) for $MgAl_2O_4$(MAO)

Multilayer structure

Annealed @350-450℃

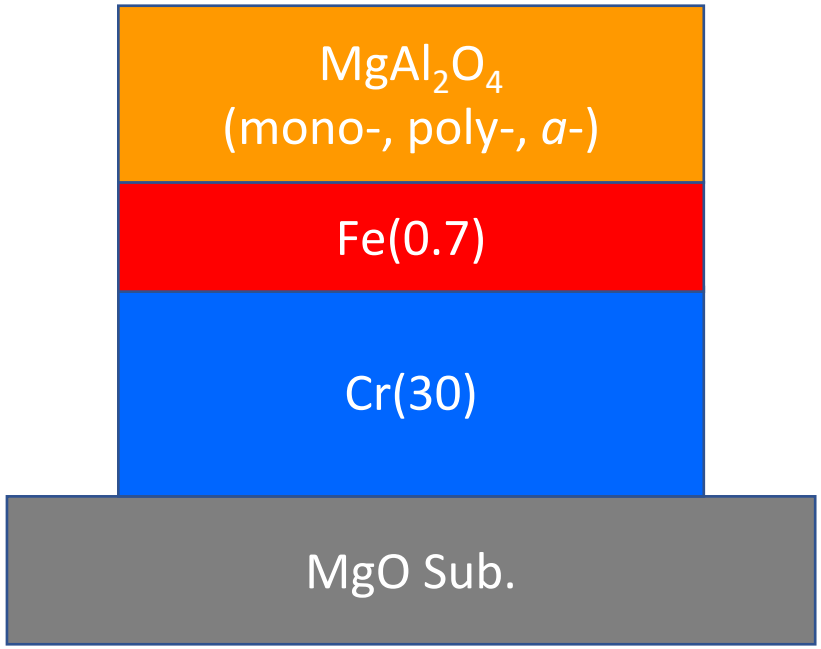

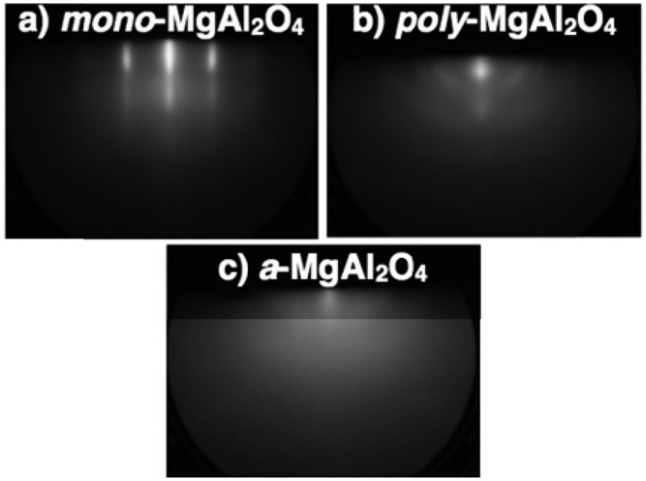

Lattice mismatch between
bcc-Fe and $MgAl_2O_4$ is 0.2%.

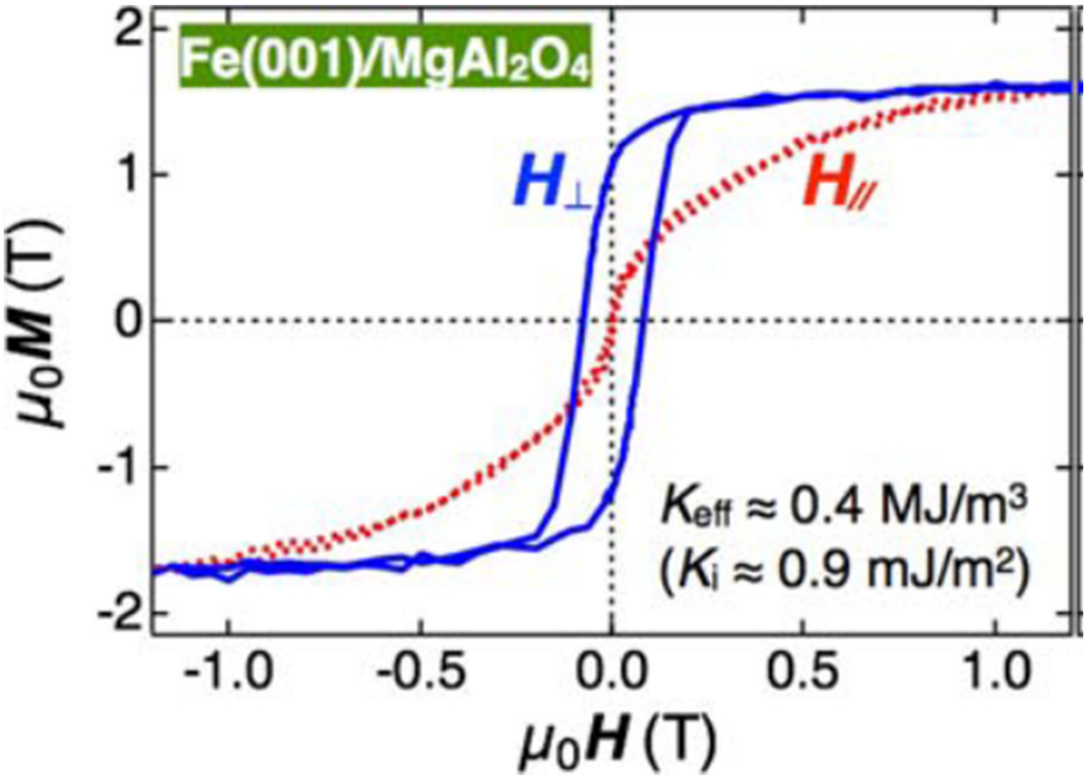

J. Koo, *et.al.*, Phys. status solidi RRL **8**, 841 (2014).

Ki of Fe/MgO(001) is 1.4mJ/m2,
J. W. Koo, *et al.*, Appl. Phys. Lett. 103, 192401 (2013).

Purpose of this work

We study interfacial magnetocrystalline anisotropy (MAE) in Fe/MgAl2O4 and Fe/MgO by means of first-principles calculations based on density functional theory.

$Fe/MgAl_2O_4(2a_{Fe})$ $Fe/MgO\ (a_{Fe},a_{MgO})$

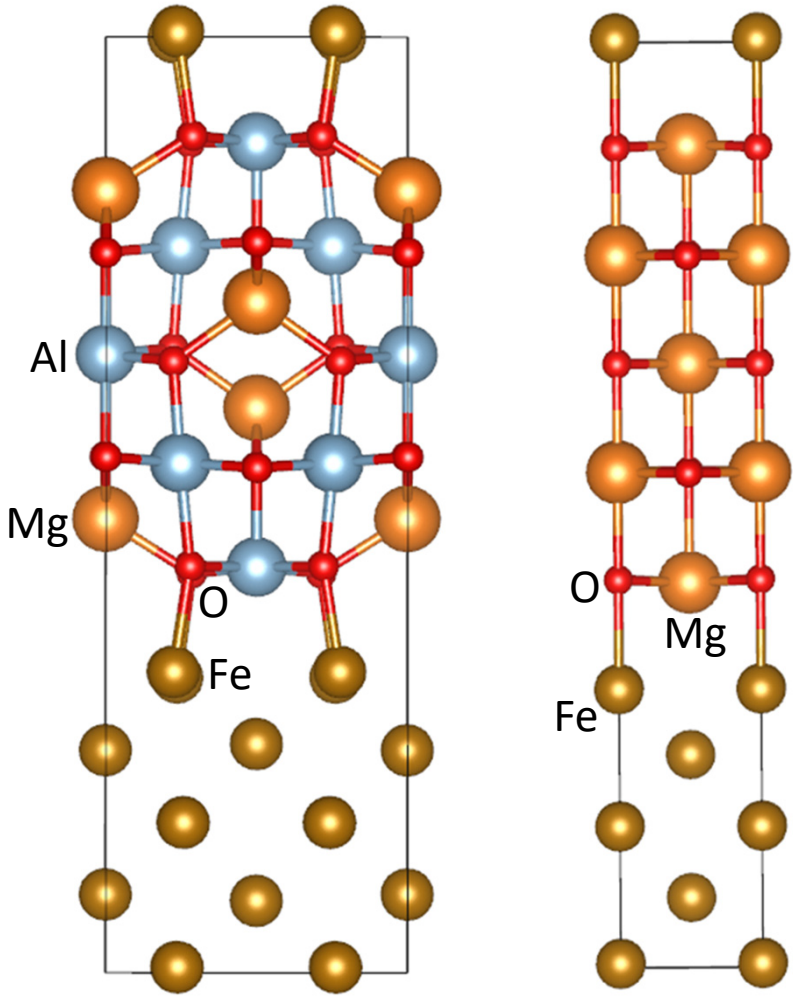

・origin of interfacial perpendicular magnetocrystalline anisotropy (PMA)

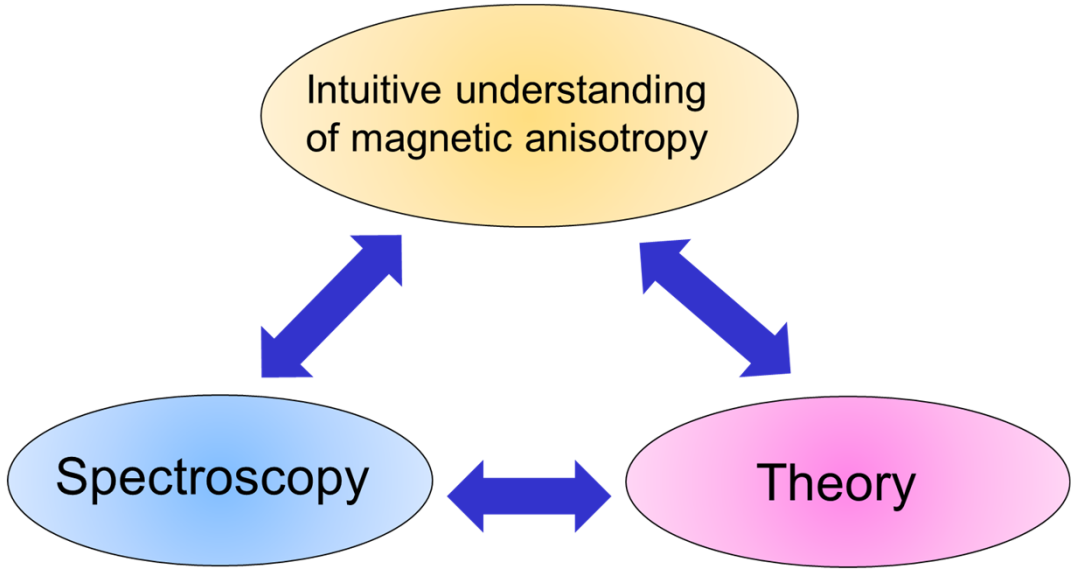

・XMCD Measurement (orbital and spin moment , quadrupole moment)

・First-principles calculations
・2nd order perturbation of SOI

PMA energy for $Fe/MgAl_2O_4$(MAO) and Fe/MgO

Fe/MgO(001)
($a_{||}=a_{Fe}$)

$Fe/MgAl_2O_4$(MAO)(001)
($a_{||}=2a_{Fe}$)

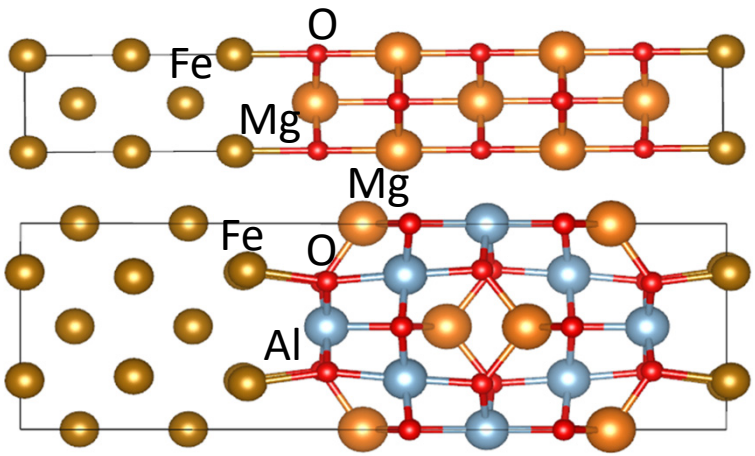

K. Masuda and Y. Miura, PRB **98**, 224421 (2018).

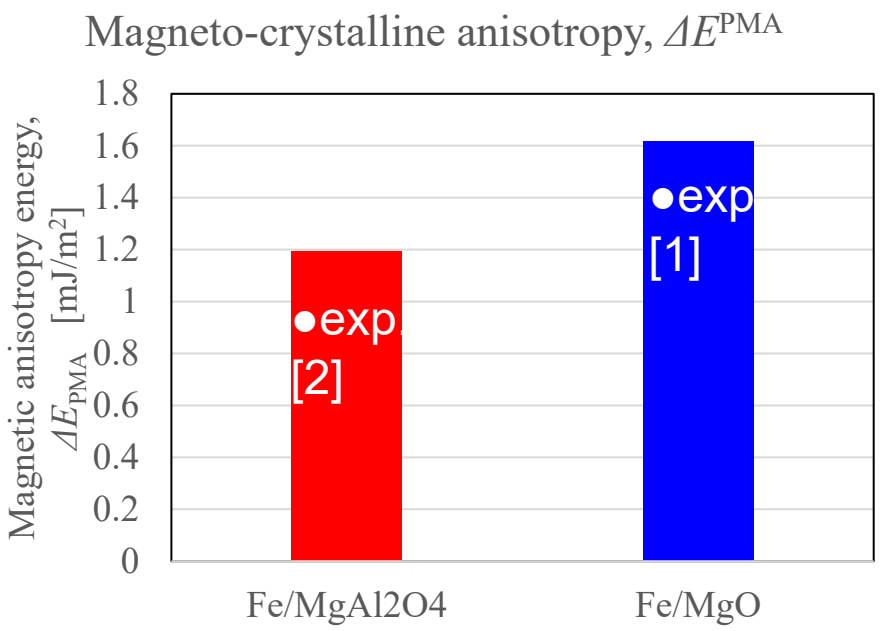

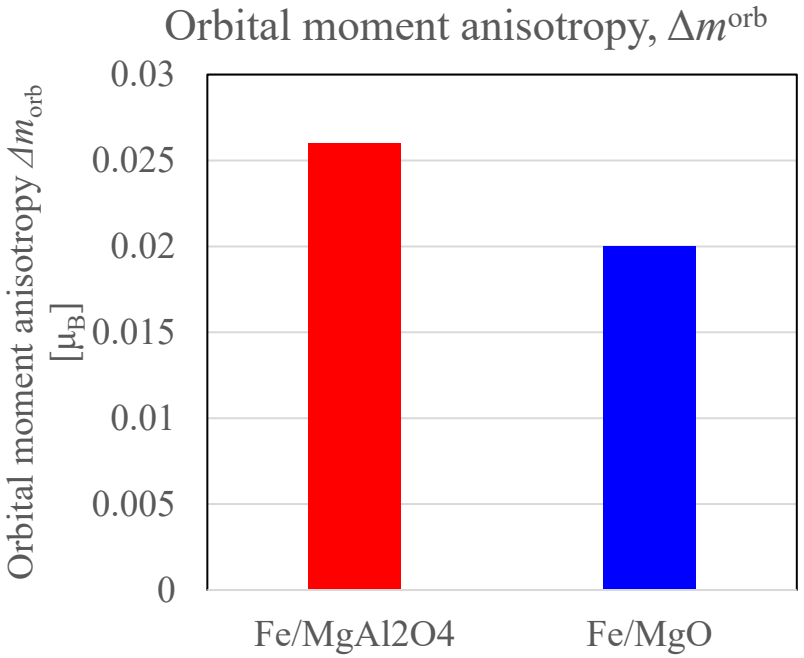

[1] J. W. Koo, *et al.*, Appl. Phys. Lett. 103, 192401 (2013).

[2] J. W. Koo, *et.al.*, Phys. status solidi RRL **8**, 841 (2014).

$$\Delta E^{\mathrm{PMA}} \approx \frac{\xi}{4\mu_{\mathrm{B}}}\left(\Delta m^{\mathrm{orb}}\right) + \frac{21}{2\mu_{\mathrm{B}}}\frac{\xi^2}{\Delta E_{\mathrm{ex}}}\left(\Delta m^{T}\right)$$

Second order perturbation of spin-orbit interaction (SOI)

P. Bruno, PRB **39**, 865 (1989).
G. Laan, JPCM **10**, 3239 (1998).

$$\delta E = -\sum_{\text{exc}} \frac{\left|\langle \text{exc}|H^{\text{SO}}|\text{gr}\rangle\right|^2}{\varepsilon_{\text{exc}} - \varepsilon_{\text{gr}}}$$

$$H^{\text{SO}} = \xi \vec{L} \cdot \vec{S}$$

$$|\text{gr (exc)}\rangle = \sum_{\mu,\sigma} c_{i,\mu,\sigma}\, |i,\mu\rangle$$

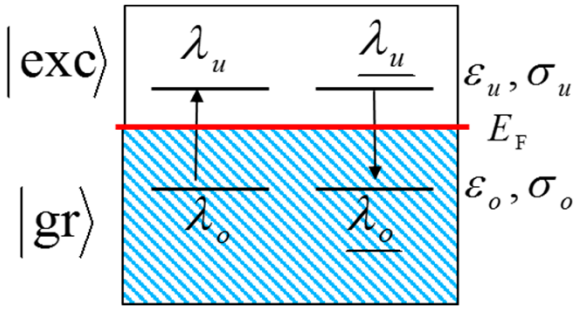

μ : local atomic orbital index
i,j : index of atomic position

Perpendicular magneto-crystalline anisotropy (PMA) energy

$$\Delta E^{\text{PMA}} = \delta E[\text{in-plane}] - \delta E[\text{perpendicuar}]$$

$$\Delta E^{\text{PMA}}(i) = \sum_{\sigma,\sigma'} (-1)^{\delta_{\sigma'\sigma}} \xi_i^2 \sum_{o,\,u} \frac{|\langle o,\sigma'|L_z|u,\sigma,i\rangle|^2 - |\langle o,\sigma'|L_x|u,\sigma,i\rangle|^2}{\varepsilon_{u,\sigma'} - \varepsilon_{o,\sigma}}$$

$$= \Delta E^{\text{PMA}}_{\uparrow\Rightarrow\uparrow}(i) + \Delta E^{\text{PMA}}_{\downarrow\Rightarrow\downarrow}(i) + \Delta E^{\text{PMA}}_{\uparrow\Rightarrow\downarrow}(i) + \Delta E^{\text{PMA}}_{\downarrow\Rightarrow\uparrow}(i)$$

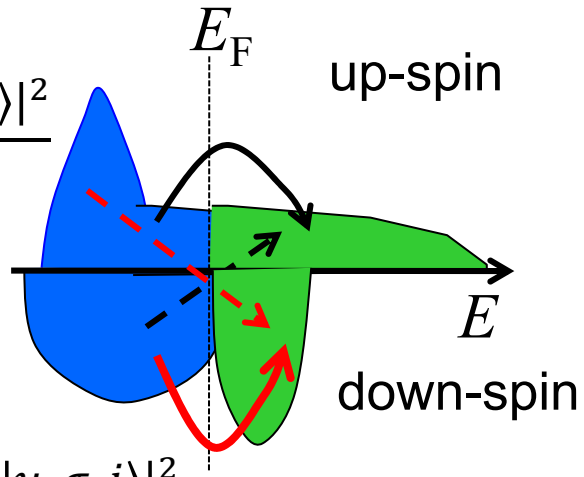

Orbital moment $\quad \langle L^z \rangle = 4\xi_i \sum_{o,\,u} \frac{|\langle o,\uparrow|L_z|u,\uparrow,i\rangle|^2 - |\langle o,\downarrow|L_z|u,\sigma,i\rangle|^2}{\varepsilon_{u,\sigma'} - \varepsilon_{o,\sigma}}$

Spin-decomposed PMA energy of Fe/$MgAl_2O_4$(MAO) and Fe/MgO

Fe/$MgAl_2O_4$(MAO) $a=a_{Fe}$

$\Delta E^{PMA}=1.2[mJ/m^2]$

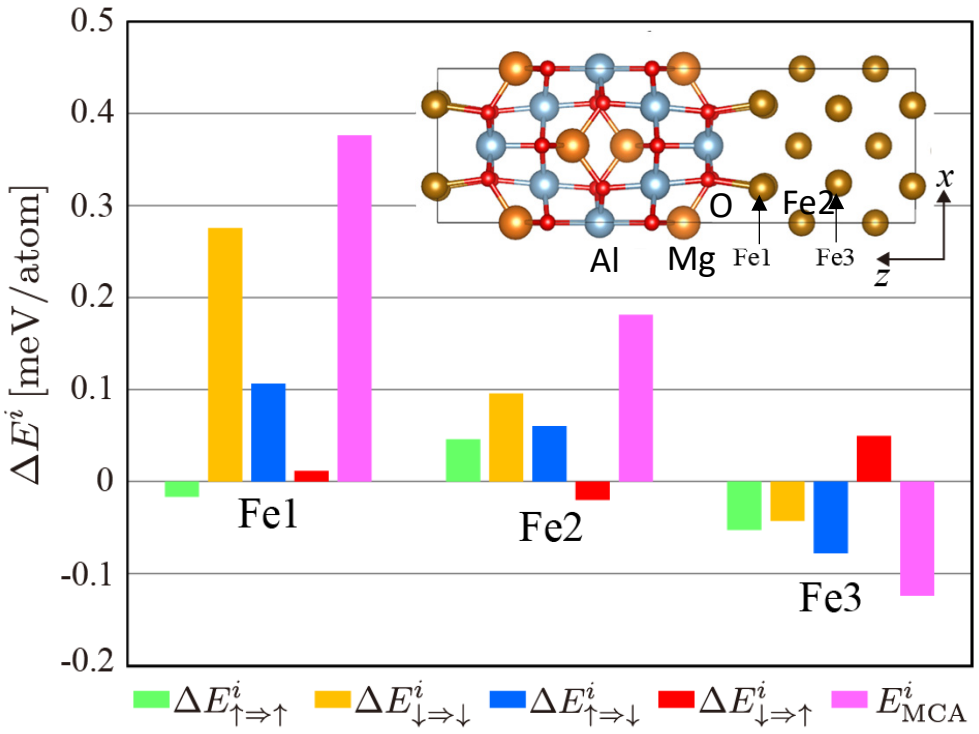

Fe/MgO $a=a_{Fe}$

$\Delta E^{PMA}=1.6[mJ/m^2]$

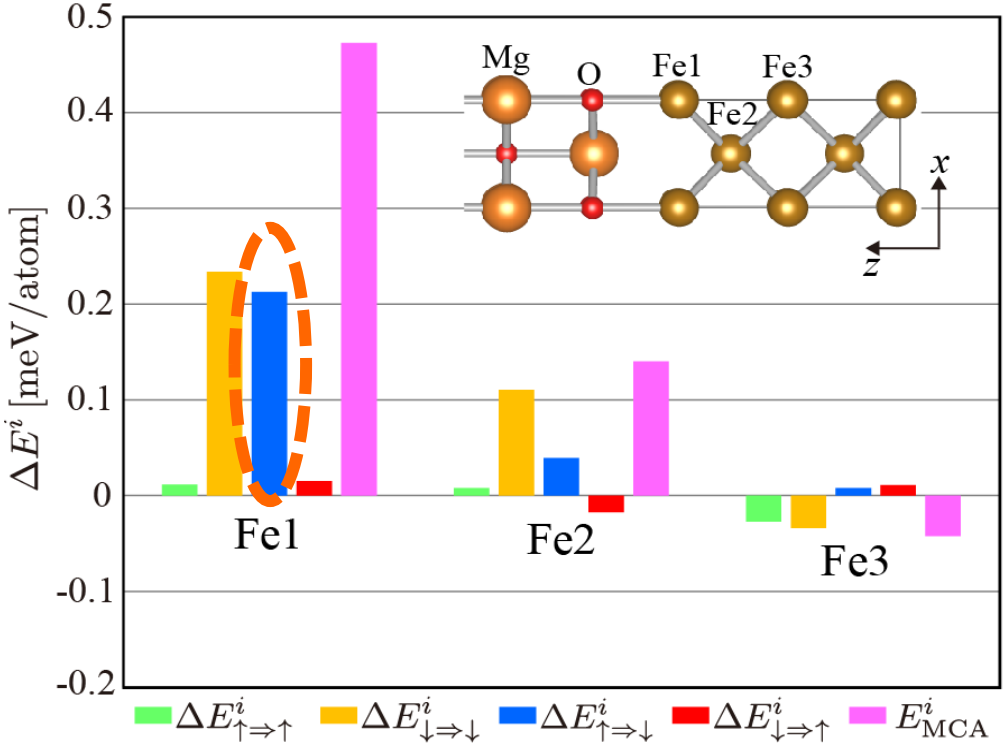

- Interfacial Fe mainly contributes to PMA
- Spin conservation term $\Delta E^{PMA}_{\downarrow\Rightarrow\downarrow}(i)$ mainly contributes to PMA.
- For Fe/MgO, the spin flip term $\Delta E^{PMA}_{\uparrow\Rightarrow\downarrow}(i)$ also contributes to PMA.

Spin conserving term and spin flip term in magnetic anisotropy

Spin conserving term $\Delta E^{\mathrm{PMA}}_{\downarrow\Rightarrow\downarrow}(i) = +\xi_i^2 \sum_{o,\,u} \frac{|\langle u,\downarrow|L_z|o,\downarrow,i\rangle|^2}{\varepsilon_{u,\downarrow}-\varepsilon_{o,\downarrow}} - \xi_i^2 \sum_{o,\,u} \frac{|\langle u,\downarrow|L_x|o,\downarrow,i\rangle|^2}{\varepsilon_{u,\downarrow}-\varepsilon_{o,\downarrow}}$

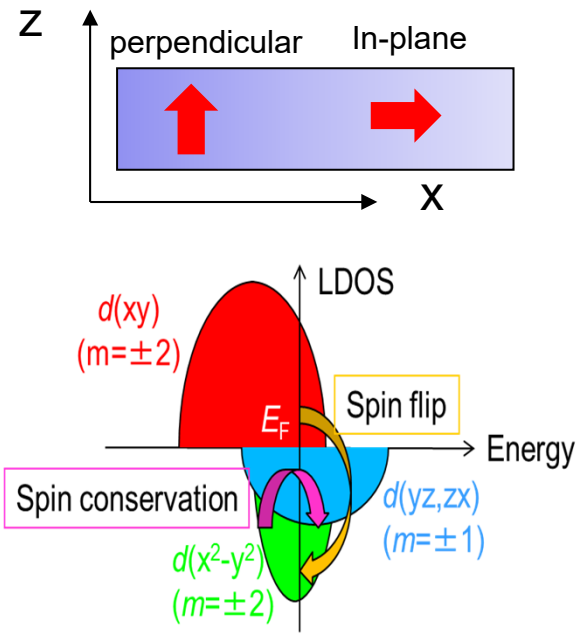

$L_z Y_l^m = m Y_l^m$

Contributed to PMA energy, if there are *d* orbitals with the same magnetic quantum number *m* exist around E_F.

$\langle zx,\downarrow|L_z|yz,\downarrow\rangle = 1$

$\langle x^2-y^2,\downarrow|L_z|xy,\downarrow\rangle = 2$

$L_x Y_l^m \propto Y_l^{m\pm1}$

Contributed to PMA energy, if there are *d* orbitals with *m* and m±1 exist around E_F.

$\langle xy,\downarrow|L_x|zx,\downarrow\rangle = 1$

$\langle x^2-y^2,\downarrow|L_x|zx,\downarrow\rangle = 1$

$\langle 3z^2-r^2,\downarrow|L_x|yz,\downarrow\rangle = \sqrt{3}$

Spin flip term $\Delta E^{\mathrm{PMA}}_{\downarrow\Rightarrow\uparrow}(i) = -\xi_i^2 \sum_{o,\,u} \frac{|\langle u,\uparrow|L_z|o,\downarrow,i\rangle|^2}{\varepsilon_{u,\uparrow}-\varepsilon_{o,\downarrow}} + \xi_i^2 \sum_{o,\,u} \frac{|\langle u,\uparrow|L_x|o,\downarrow,i\rangle|^2}{\varepsilon_{u,\uparrow}-\varepsilon_{o,\downarrow}}$

2nd order perturbation energy

G. der Laan, JPCM 10, 3239 (1998).

$$\delta E \approx -\frac{1}{4}\xi \hat{\boldsymbol{S}}\cdot[\langle \boldsymbol{L}_\downarrow\rangle - \langle \boldsymbol{L}_\uparrow\rangle] + \frac{\xi^2}{\Delta E_{\mathrm{ex}}}\left[\frac{21}{2}\hat{\boldsymbol{S}}\cdot\langle \boldsymbol{T}\rangle + 2\left\langle \left(L_\varsigma S_\varsigma\right)^2\right\rangle\right]$$

Orbital moment term
(Spin-conserving term)

Magnetic dipole term
(Spin-flip and spin-conserving term)

Intuitive understanding of magneto-crystalline anisotropy

P. Bruno, PRB **39**, 865 (1989).
G. Laan, JPCM **10**, 3239 (1998).

$$\Delta E^{\mathrm{PMA}} \approx \frac{\xi}{4\mu_{\mathrm{B}}}\left(\Delta m^{\mathrm{orb}}\right) + \frac{21}{2\mu_{\mathrm{B}}}\frac{\xi^2}{\Delta E_{\mathrm{ex}}}\left(\Delta m^{T}\right)$$

Orbital moment term

Magnetic dipole term

$$\Delta m^{\mathrm{orb}} = \langle L^z \rangle - \langle L^x \rangle$$

$$\Delta m^{T} = \langle T^z \rangle - \langle T^x \rangle$$

Orbital moment term

$$H^{\mathrm{SO}} = -\xi \vec{L} \cdot \vec{S}$$

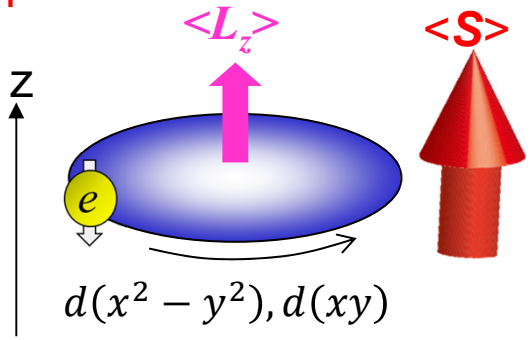

Perpendicular magnetic anisotropy

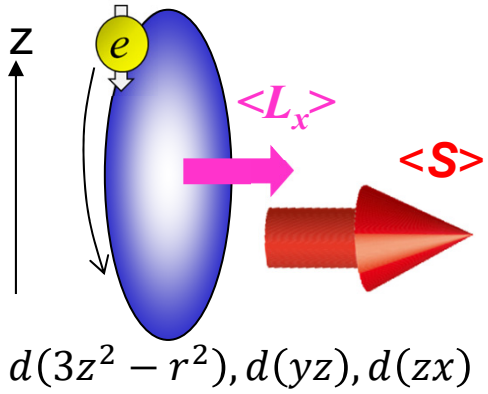

In-plane magnetic anisotropy

Magnetic dipole term *T* ⇒Quadrupole moment of spin density

$$\vec{T} \approx -\frac{2}{7}\boldsymbol{Q}\hat{S} \quad \Rightarrow \quad T^z \approx -\frac{2}{7}\sum_{i=1}^{5} Q_i^z S^i$$

Q: Quadrupole moment of spin density

$Q^z < 0$ ($T^z > 0$)⇒ Prolate distribution

$Q^z > 0$ ($T^z < 0$) ⇒ Oblate distribution

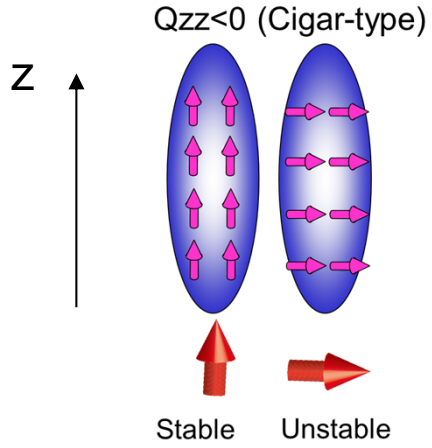

Perpendicular magnetic anisotropy

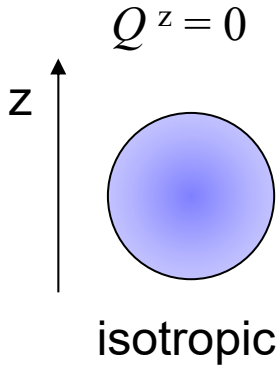

isotropic

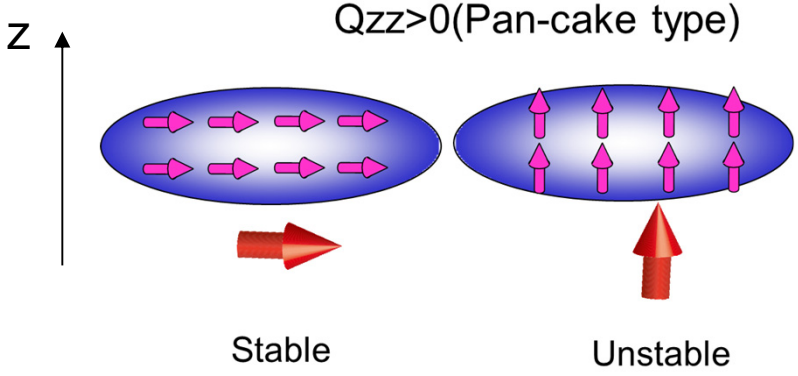

In-plane magnetic anisotropy

Magnetic dipole term of $Fe/MgAl_2O_4$ and Fe/MgO

$$m^T = T^z \approx -\frac{2}{7}\left(-16m^{3z^2-r^2} - 8m^{zx} - 8m^{yz} + 16m^{xy} + 16m^{x^2-y^2}\right)$$

J. Stöhr and H. König, PRL **75**, 3748 (1995).

$$\Delta m^T = \frac{3}{2}\langle T^z \rangle$$

Quadrupole distribution of *d* orbitals

Orbital i	$\alpha = x, y$ or z $4\left(7\,Q_\alpha^i\right)$
d_{yz}	−8, −8, 16
d_{xz}	−8, 16, −8
$d_{3z^2-r^2}$	−16, 8, 8
d_{xy}	16, −8, −8
$d_{x^2-y^2}$	16, −8, −8

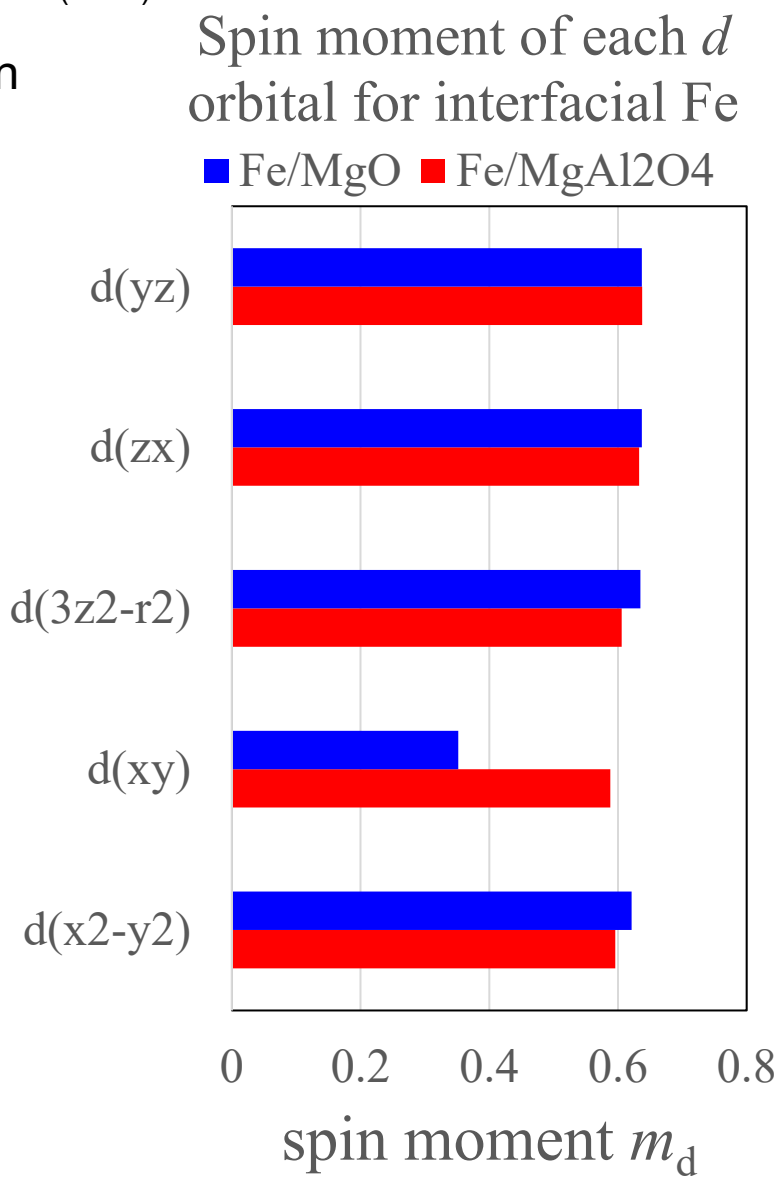

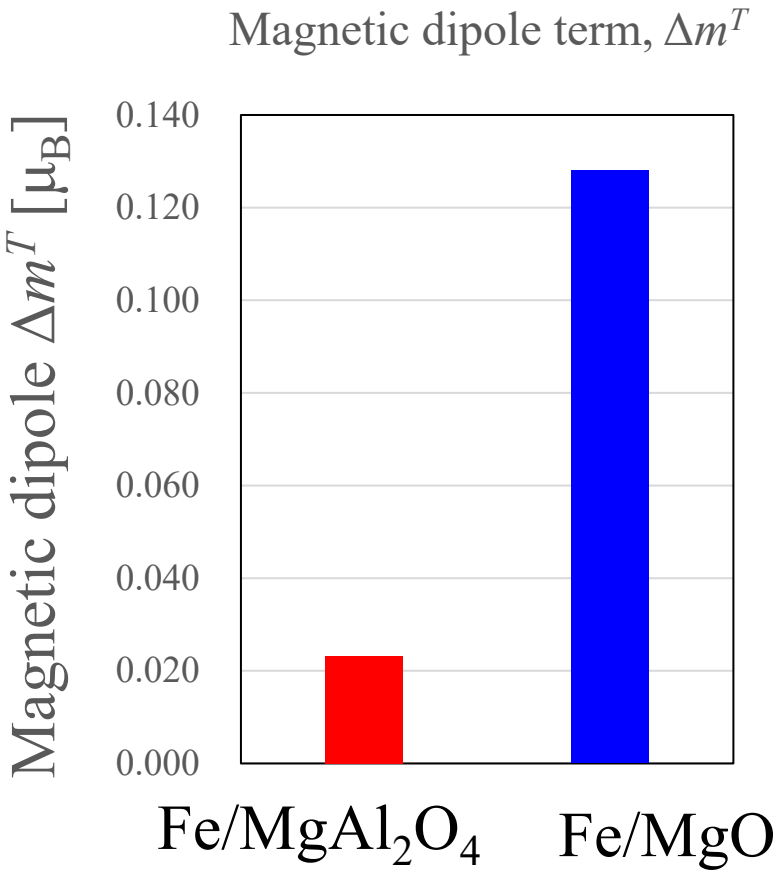

Magnetic dipole term of $Fe/MgAl_2O_4$ and Fe/MgO

$$\langle T^z \rangle \approx -\frac{2}{7}\sum_{i=1}^{5} Q_i^z S^i = -\frac{2}{7}\left(-16m^{3z^2-r^2} - 8m^{zx} - 8m^{yz} + 16m^{xy} + 16m^{x^2-y^2}\right)/16$$

J. Stöhr and H. König, PRL **75**, 3748 (1995).

$$\Delta m^T = \frac{3}{2}\langle T^z \rangle$$

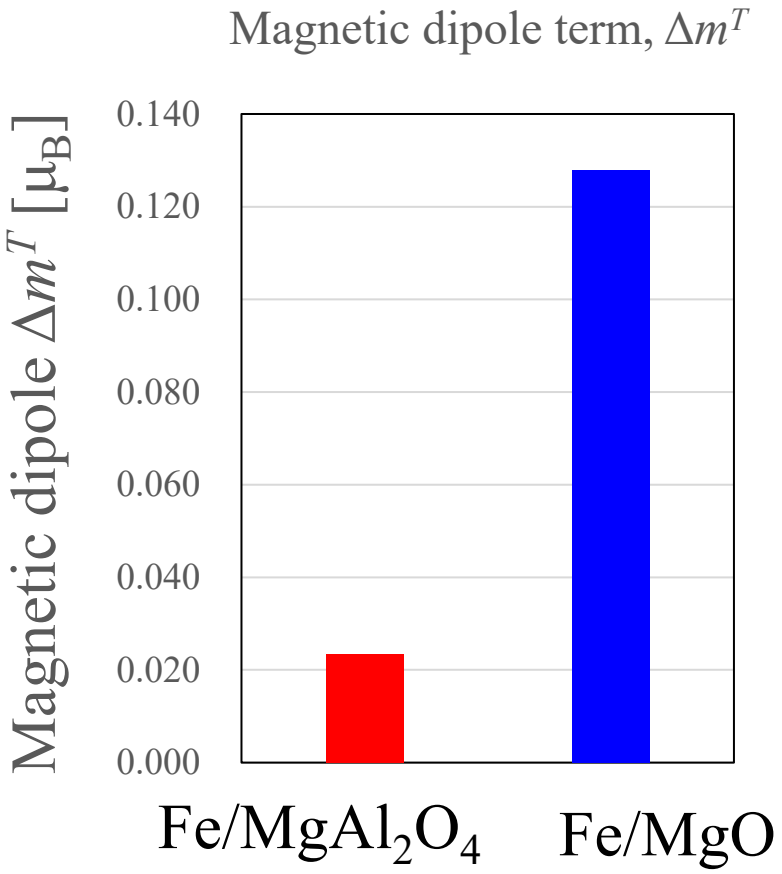

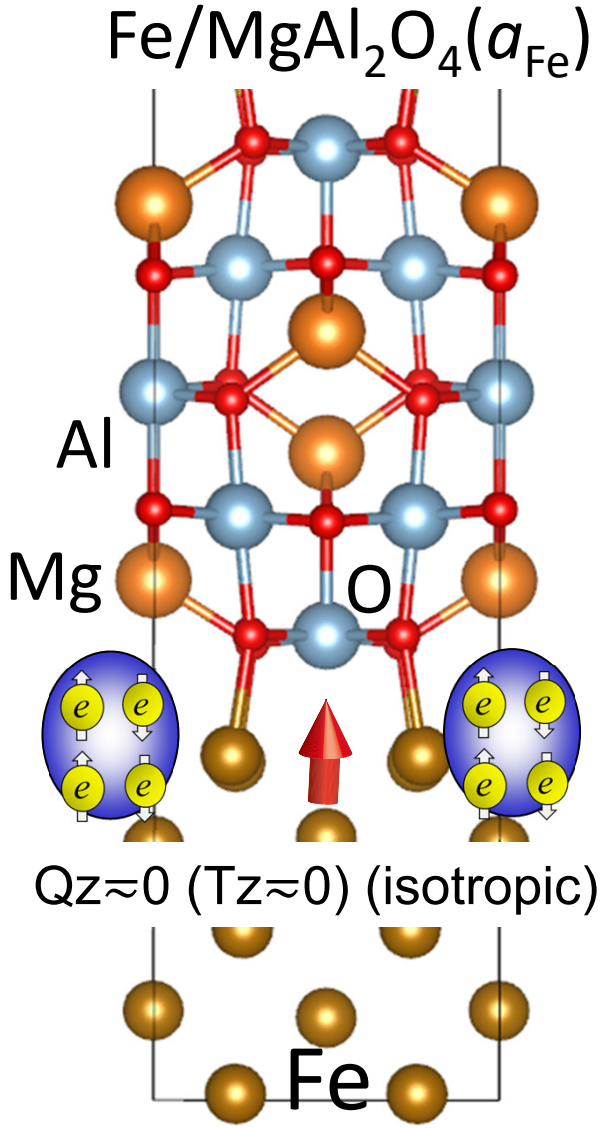

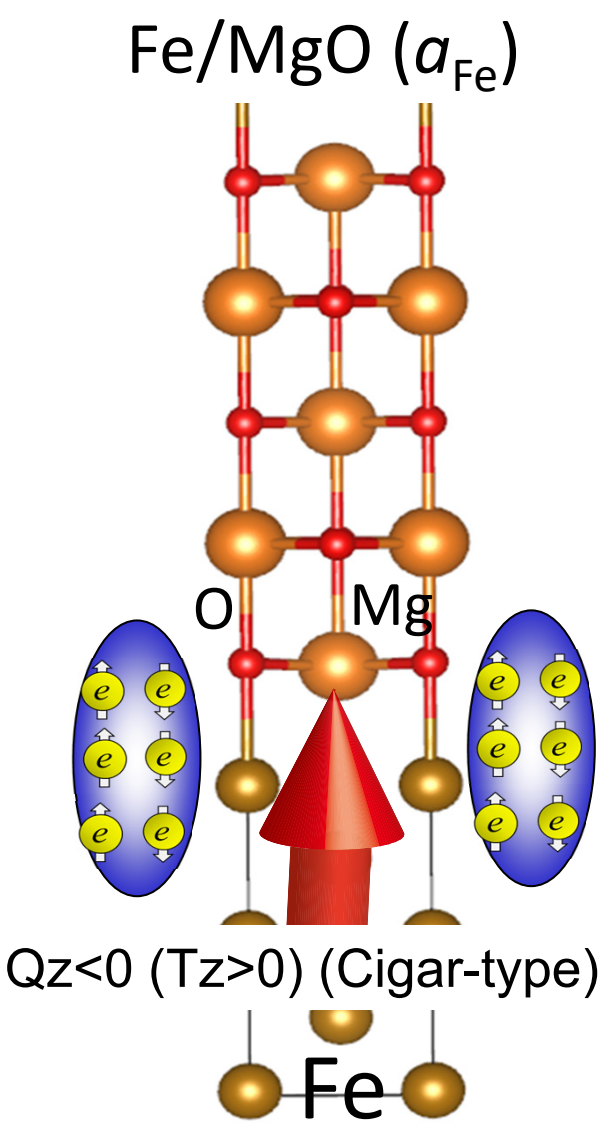

Summary of the second topic

- $Fe/MgAl_2O_4(001)$ show PMA, which is slightly smaller than that of Fe/MgO(001).

- For Fe/MgO(001), not only spin conservation term $\Delta E_{\downarrow\Rightarrow\downarrow}$ but also spin-flip term $\Delta E_{\uparrow\Rightarrow\downarrow}$ contributes to PMA, resulting in larger PMA than that of $Fe/MgAl_2O_4$.

- Cigar type quadrupole moment additionally increases the PMA of Fe/MgO, but not for $Fe/MgAl_2O_4$(MAO).

The quadrupole moment of spin-density is essential to understand the magneto-crystalline anisotropy especially for ferromagnetic interfaces.

Topics

0. Introduction on spintronics

1. First-Principles Study on magneto-crystalline anisotropy of Fe/MgO(001) and Fe/$MgAl_2O_4$(001)

K. Masuda and Y. Miura, PRB **98**, 224421 (2018).

2. First-Principles Study on magnetic damping of Fe/MgO(001)

Y. Miura, in preparation

3. First-Principles Study on magneto Seebeck Effect in magnetic tunnel junctions

K. Yamamoto, K. Masuda, K. Uchida, Y. Miura arXiv:1912.01207

Voltage-driven dynamic switching in MTJ

Applied Physics Express **9**, 013001 (2016)
http://doi.org/**10.7567/APEX.9.013001**

Evaluation of write error rate for voltage-driven dynamic magnetization switching in magnetic tunnel junctions with perpendicular magnetization

Yoichi Shiota*, Takayuki Nozaki, Shingo Tamaru, Kay Yakushiji, Hitoshi Kubota, Akio Fukushima, Shinji Yuasa, and Yoshishige Suzuki

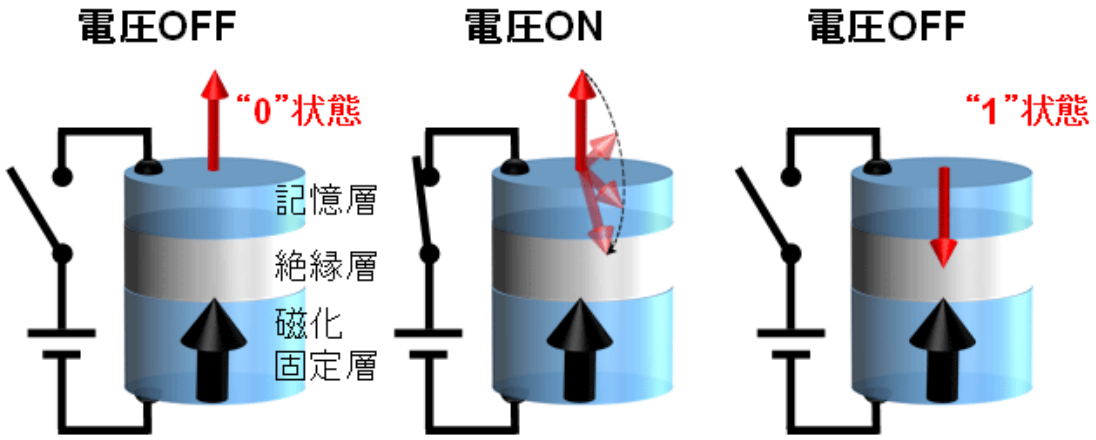

From website of Sahashi's ImPACT project in JST

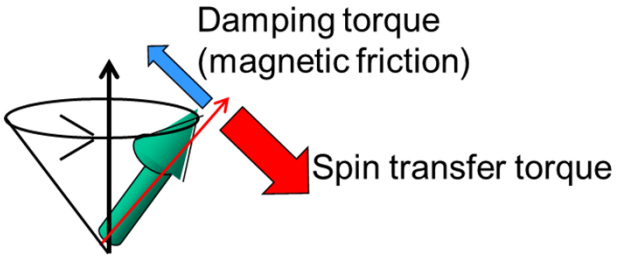

Write Error Rate (WER)

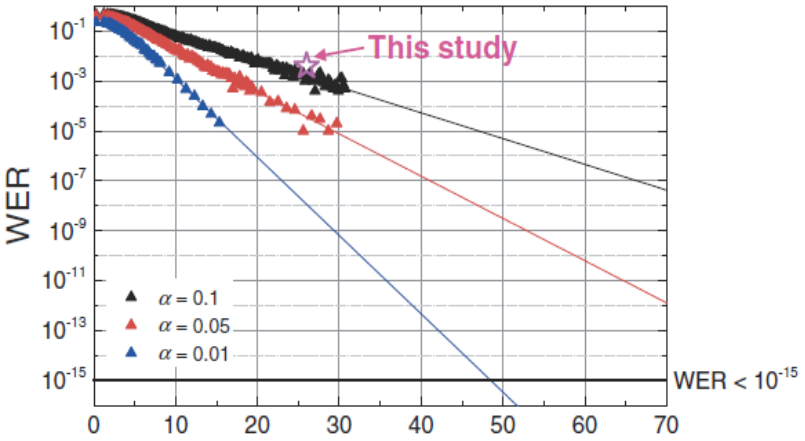

Fig. 4. Calculated WER as a function of Δ for fixed tilted magnetization angle and half precession period τ_{pulse} for various damping constants.

Pulsed bias voltage changes PMA of interface of FM layer and promote the precession motion of the magnetization.

➡ By removing the voltage with a proper pulse duration, such as a half precession period, magnetization switching can be achieved.

➡ Basically, no current flow

Large Ku and Small damping α can reduce the WER

Experiments electric field effects of PMA and magnetic damping

APPLIED PHYSICS LETTERS **105**, 052415 (2014)

Electric-field effects on magnetic anisotropy and damping constant in Ta/CoFeB/MgO investigated by ferromagnetic resonance

A. Okada,[1] S. Kanai,[1] M. Yamanouchi,[1,2] S. Ikeda,[1,2] F. Matsukura,[3,2,a)] and H. Ohno[1,2,3]
[1]*Laboratory for Nanoelectronics and Spintronics, Research Institute of Electrical Communication, Tohoku University, 2-1-1 Katahira, Aoba-ku, Sendai 980-8577, Japan*
[2]*Center for Spintronics Integrated Systems, Tohoku University, 2-1-1 Katahira, Aoba-ku, Sendai 980-8577, Japan*
[3]*WPI-Advanced Institute for Materials Research (WPI-AIMR), Tohoku University, 2-1-1 Katahira, Aoba-ku, Sendai 980-8577, Japan*

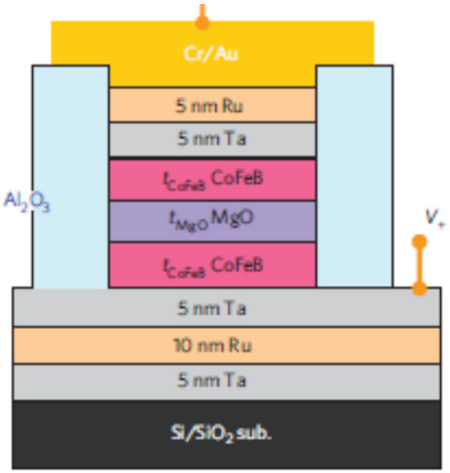

-21% of magnetic damping α is changed by 1V/nm EF for t=1.4nm

Magnetic anisotropy change by EF

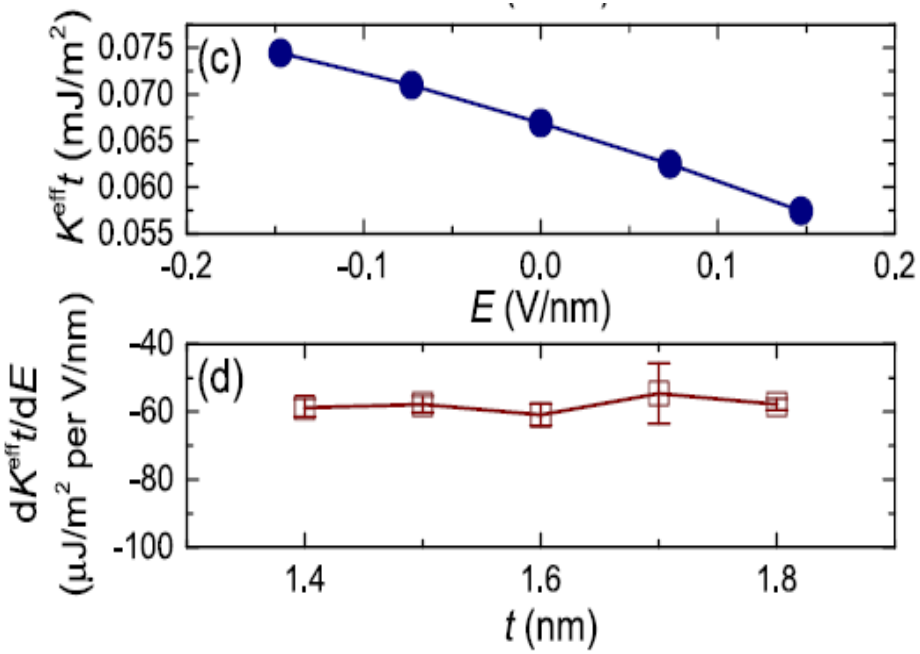

EF dependence is insensitive to thickness of FM layer

Magnetic damping change by EF

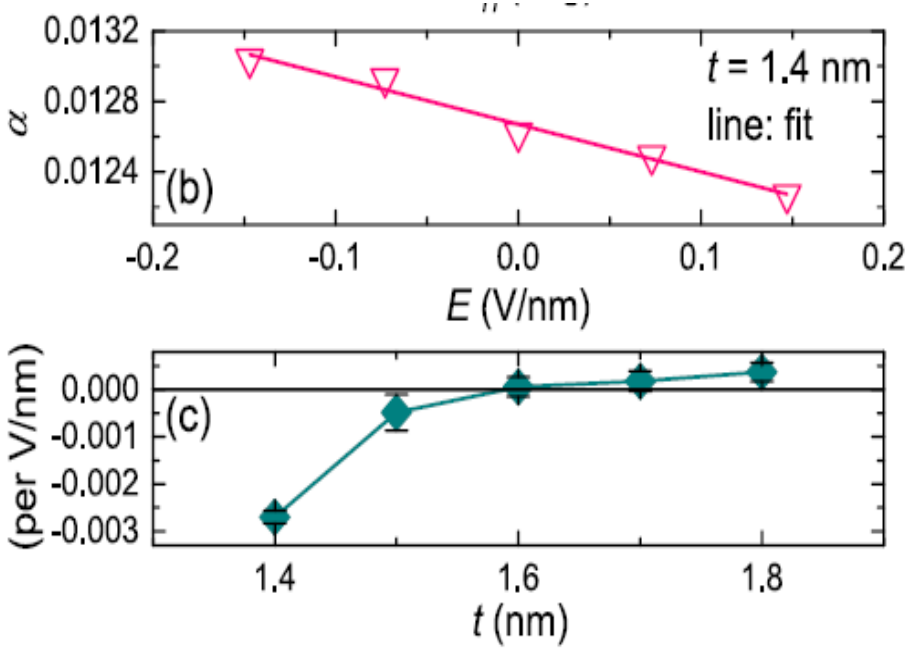

Large thickness dependence of FM layer

Purpose of this work

If PMA and magnetic damping can be simultaneously reduced by applied voltage, we can drastically reduce power consumption and write error rate in magnetization reversal of MRAM.

Voltage dependence of magnetic damping is hardly investigated.

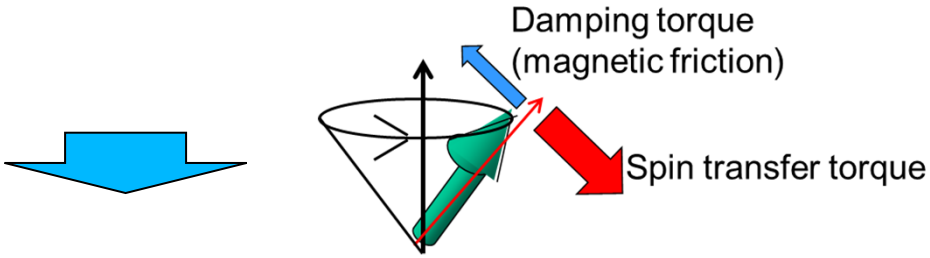

This work investigates the voltage dependence of magnetic damping and magnetic anisotropy of Fe/MgO interface based on the first-principles calculation.

Origin of Magnetic Damping α

- Electronic system
- Phonon
- Atomic disorder
- Other extrinsic factors

Kambersky's torque correlation model

V. Kambersky, Czechoslovak Journal of Physics B **26**, 1366 (1976).

Precession motion of local spin moment

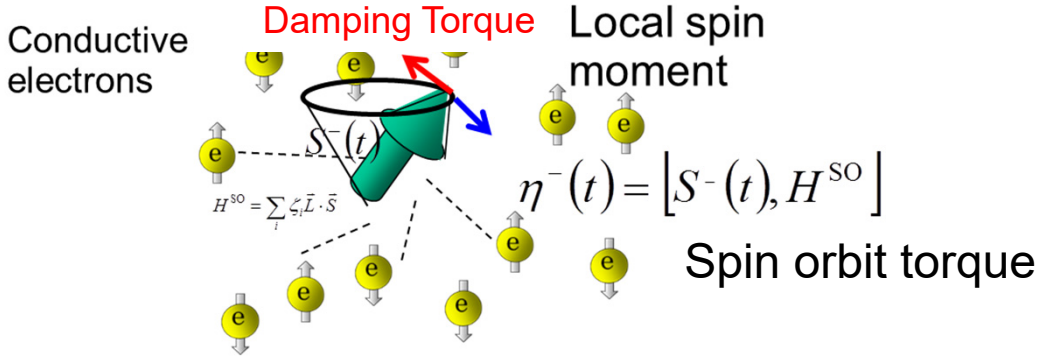

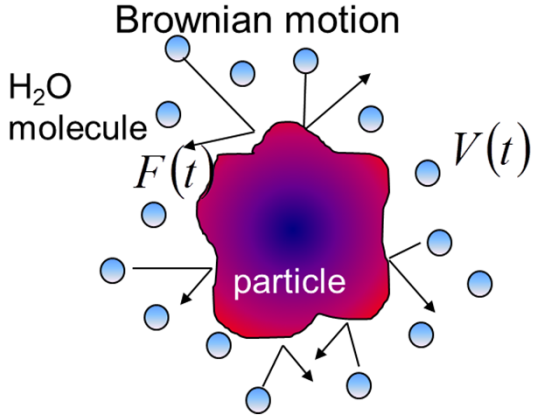

Generalized Langevin equation for magnetization dynamics

$$\frac{dS^-(t)}{dt} = \underbrace{-i\Omega S^-(t)}_{\text{Precession-tem}} \underbrace{- i\eta^-(t)}_{\text{Spin-torque term from SOI}} \underbrace{- \int_0^t P^{-1}\left\langle [\eta^-(t'), \eta^+] \right\rangle_0 S^-(t)dt'}_{\text{Damping-term}}$$

Magnetic susceptibility $\chi^+(\omega) = -\frac{\mu_0 (g\mu_B)^2}{\hbar V} \frac{P}{\omega + i0 - (\Omega - \Delta) - P^{-1}F(\omega + i0)}$

Green function of Torque operator $F(\omega + i0) = -i\int_{-\infty}^{\infty} \left\langle [\eta^-(t), \eta^+] \right\rangle_0 \theta(t) e^{i(\omega+i0)t} dt$

Magnetic susceptibility from LLG equation $\chi^+(\omega) = -\frac{\gamma M_s}{\omega - \gamma H_{eff} + i\alpha\omega}$

Magnetic damping constant (comparing macroscopic formula) $\alpha = -\lim_{\omega \to 0} \frac{\gamma}{\hbar \mu_0 V M_S} \mathrm{Im}\left[\frac{1}{\omega} F(\omega + i0)\right]$

First-principles calculation of damping constant

V. Kambersky, Czechoslovak Journal of Physics B **26**, 1366 (1976).

$$\alpha = \frac{g^2 \mu_0 \mu_B^2}{\pi \hbar V \gamma M_S} \sum_{\vec{k}} \sum_{nm} \left| \Gamma_{nm}^{-}(\vec{k}) \right|^2 \frac{\delta}{\left(E_F - E_{n\vec{k}}\right)^2 + \delta^2} \frac{\delta}{\left(E_F - E_{m\vec{k}}\right)^2 + \delta^2}$$

Eigenstates at each k-point and band

$$\gamma = \mu_0 g \mu_B / \hbar$$

Matrix elements of torque operator

$$\Gamma_{nm}^{-}(\vec{k}) = \left\langle n, \vec{k} \left| \zeta \left[S^{-}, H^{SO} \right] \right| m, \vec{k} \right\rangle$$

$H_{SO} = \xi \vec{L} \cdot \vec{S}$ Spin-orbit interaction

$$\left| m, \vec{k} \right\rangle = \sum_{i,\mu,\sigma} c_{i\mu}^{\vec{k}m\sigma} \left| i\mu \right\rangle$$

matrix elements of torque operator based on the local atomic orbital

VASP code

Bulk-Fe

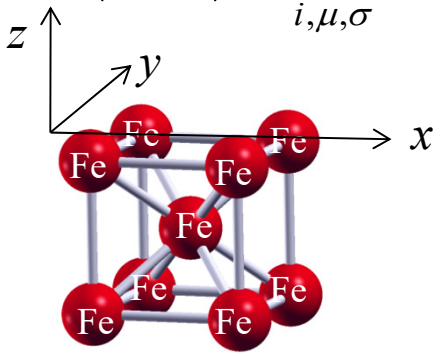

α=0.0011 (this work)

α=0.0013 (by Gilmore)

K. Gilmore, PRL **99,** 027204 (2007)

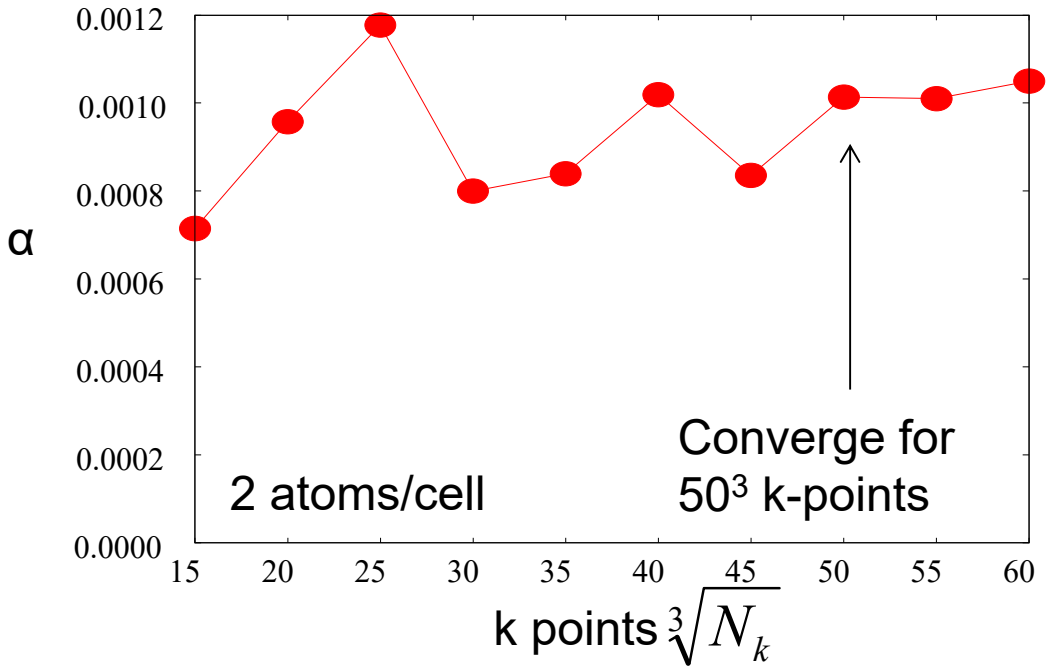

⇒For Fe/MgO(001) interface, I considered 50x50 k-points.

Potential and charge for model system

Dipole correction⇒ G. Makov and M. C. Payne, PRB **51**, 4014 (1995).

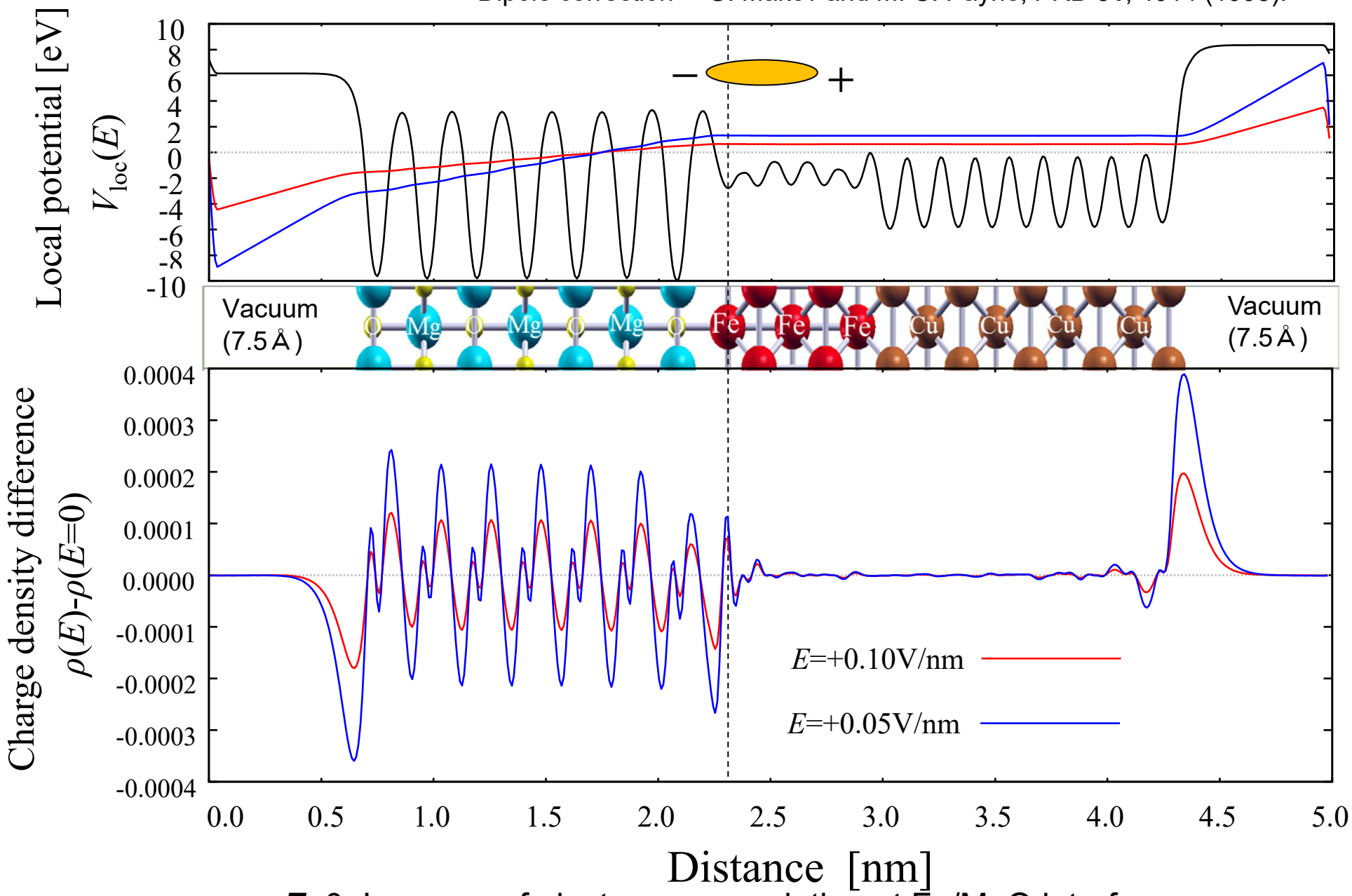

E>0 :Increase of electron accumulation at Fe/MgO interface

E<0 :Decrease of electron accumulation at Fe/MgO interface

Voltage dependence of PMA and damping α of Fe surface and Fe/MgO interface

Fe(001) surface

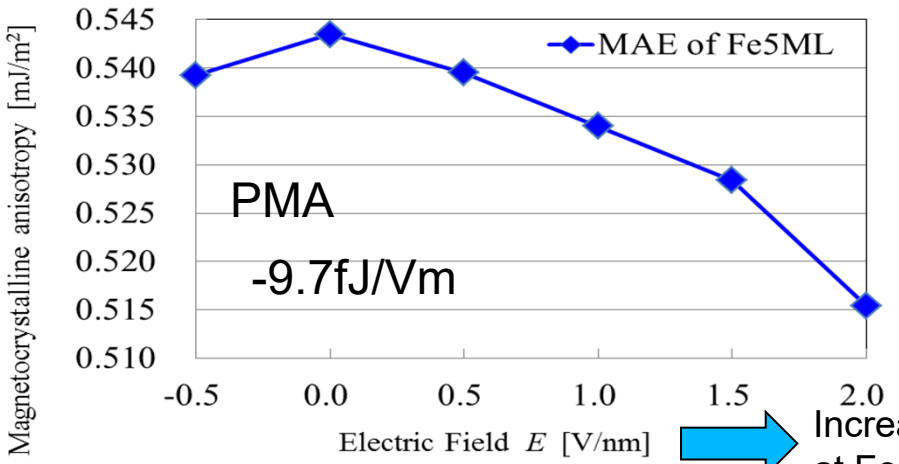

Increase of electron at Fe surface

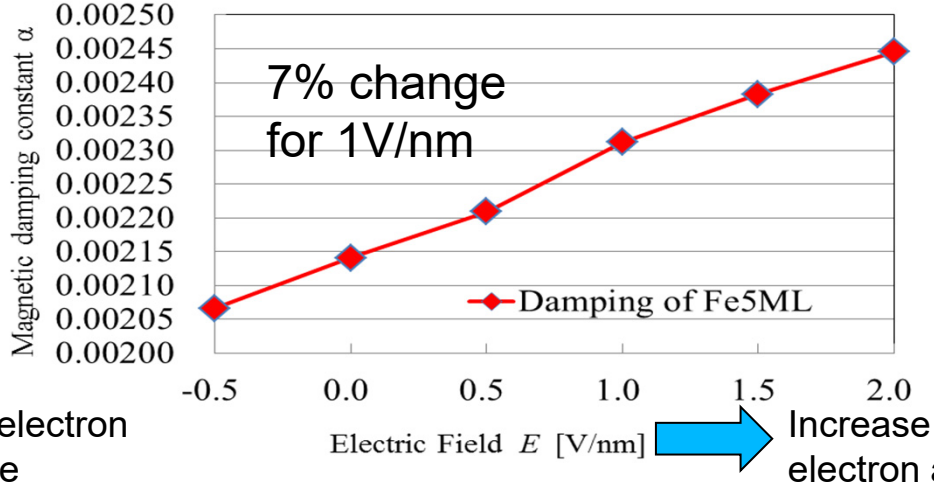

Increase of electron at Fe surface

C. G. Duan, *et al*., PRL **101**, 137201 (2008).

Fe/MgO(001) interface

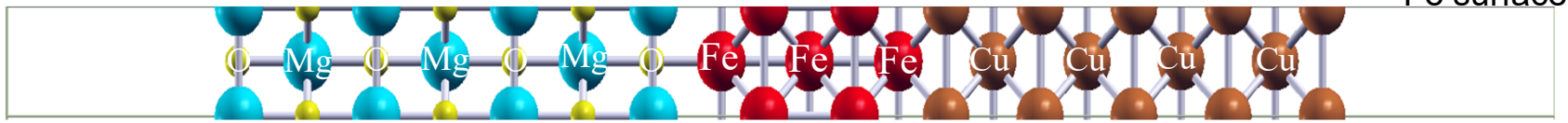

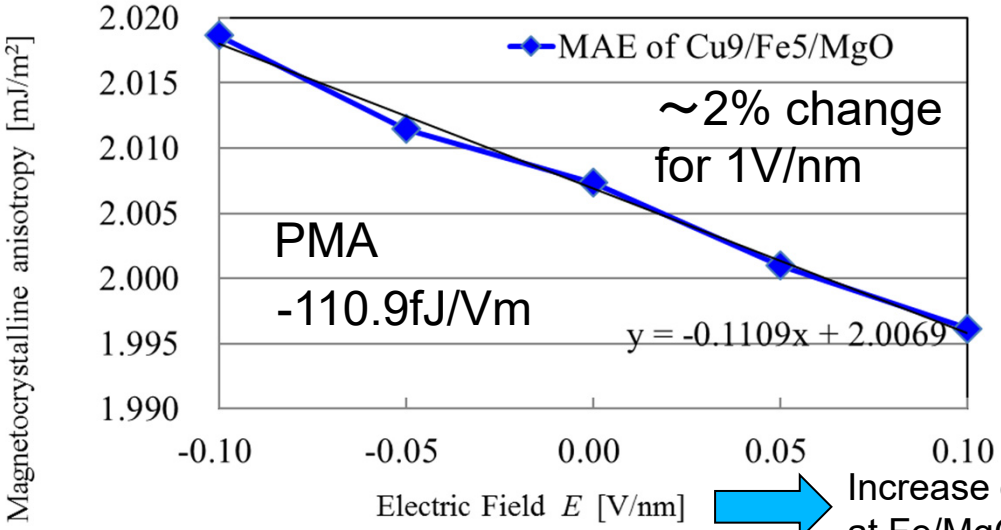

Increase of electron at Fe/MgO interface

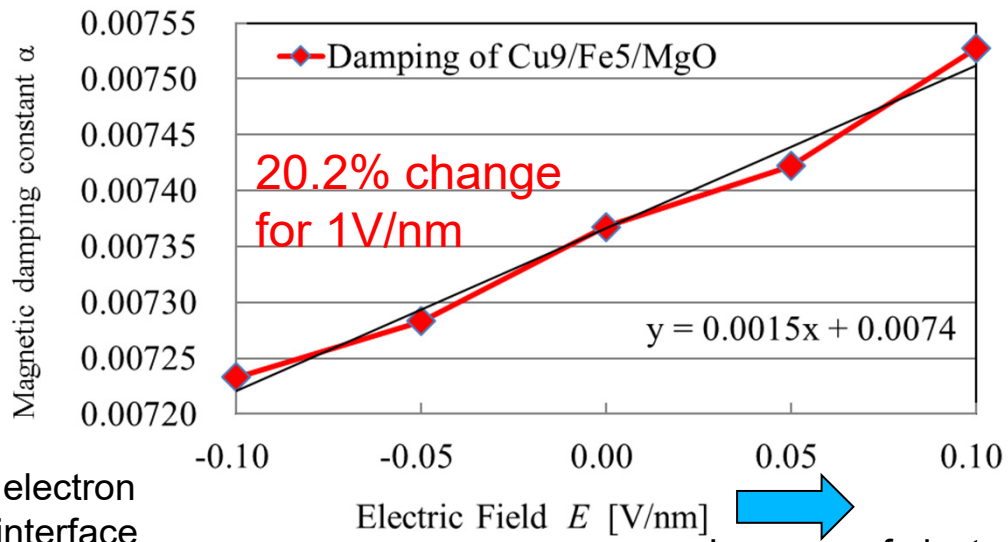

Increase of electron at Fe/MgO interface

Decomposition of magnetic damping α

Torque operator $\Gamma^- = \left[S^-, H^{SO}\right] = \zeta\left(S^z L^- - S^- L^z\right)$

Spin conservation (Orbital deexcitation) term

$\left\langle u^\sigma \left| L^- \right| o^\sigma \right\rangle$

The matrix elements are non-zero for atomic orbitals between different magnetic quantum number, such as d(yz,zx)-d(z^2), d(yz,zx)-d(x^2-y^2), d(yz,zx)-d(xy)

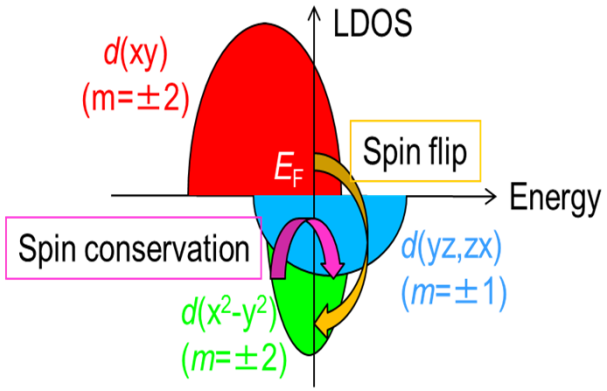

Spin flip (Orbital conservation) term

$\left\langle u^{-\sigma} \left| L_Z \right| o^\sigma \right\rangle$

The matrix elements are non-zero for atomic orbitals between same magnetic quantum number, such as d(yz)-d(zx),d(x^2-y^2)-d(xy)

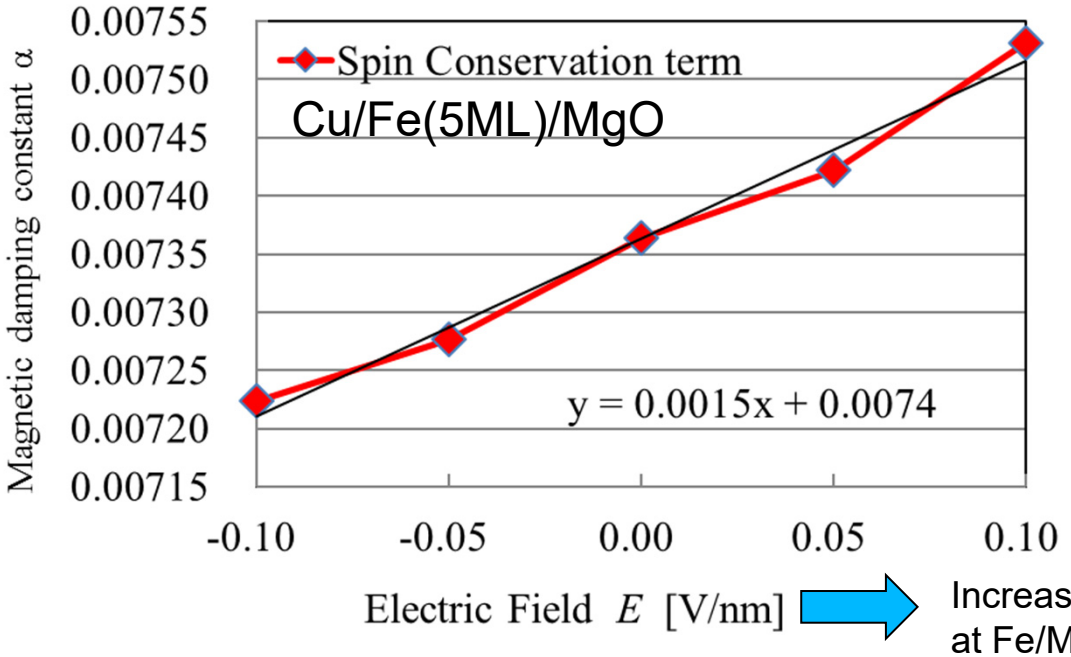

Increase of electron at Fe/MgO interface

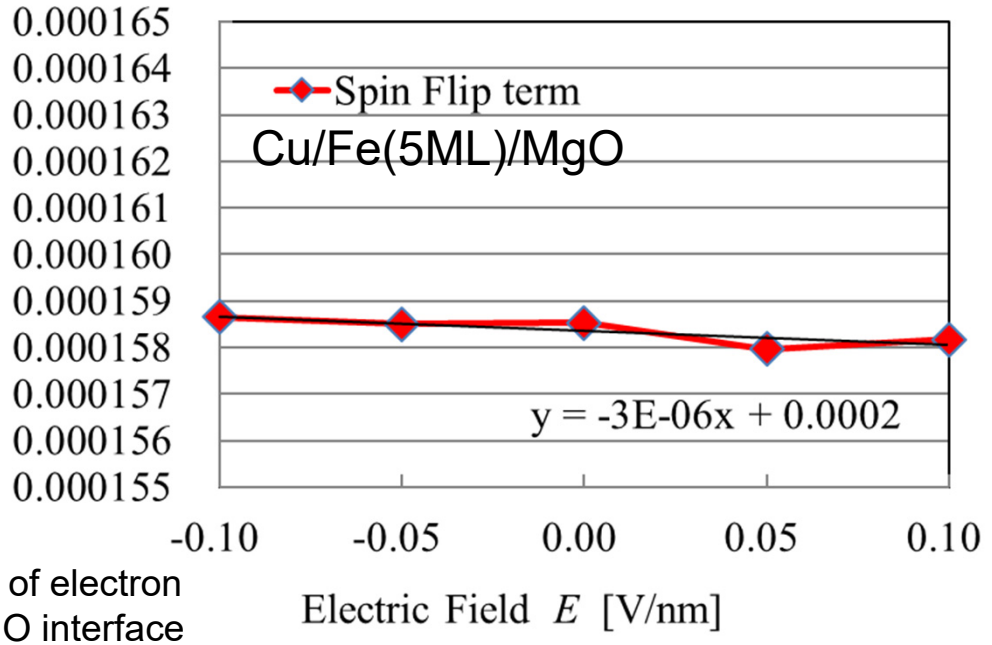

Origin of electric filed dependence

Fe/MgO(001) interface

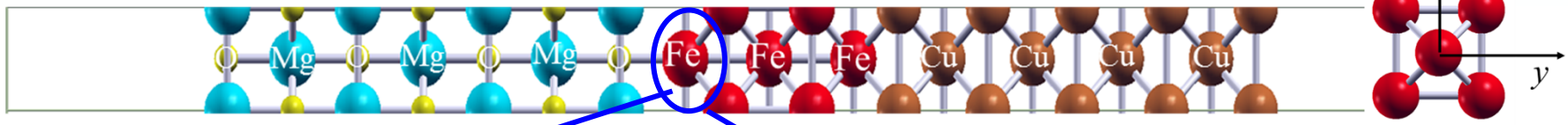

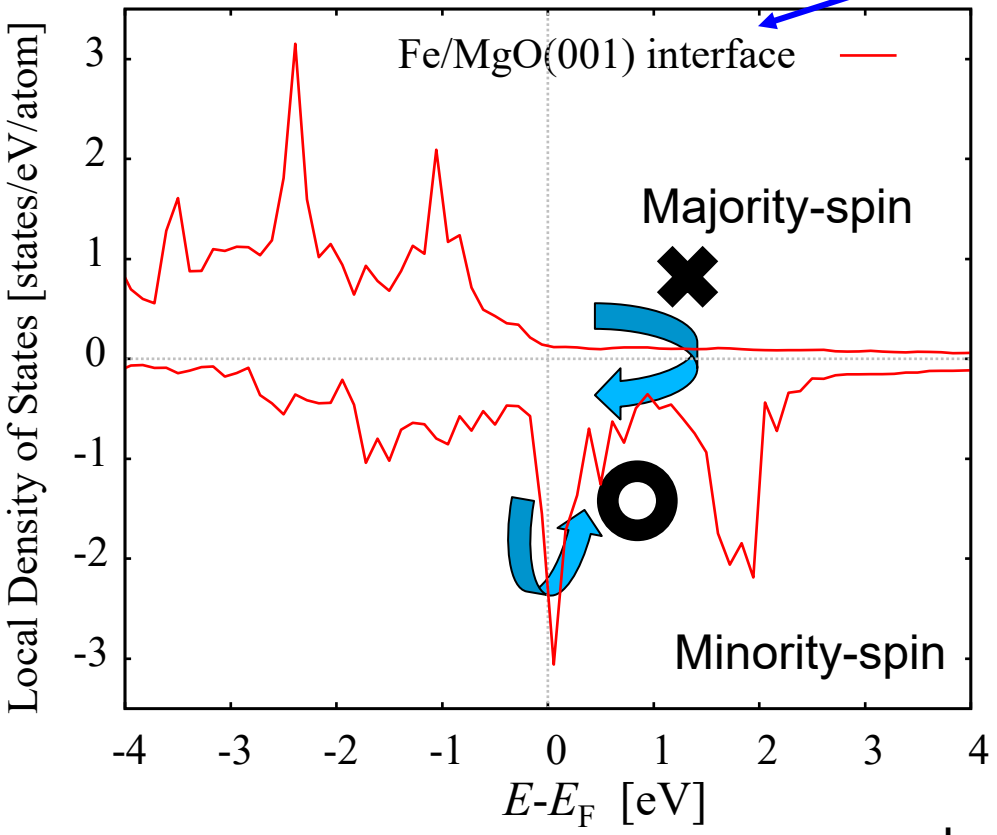

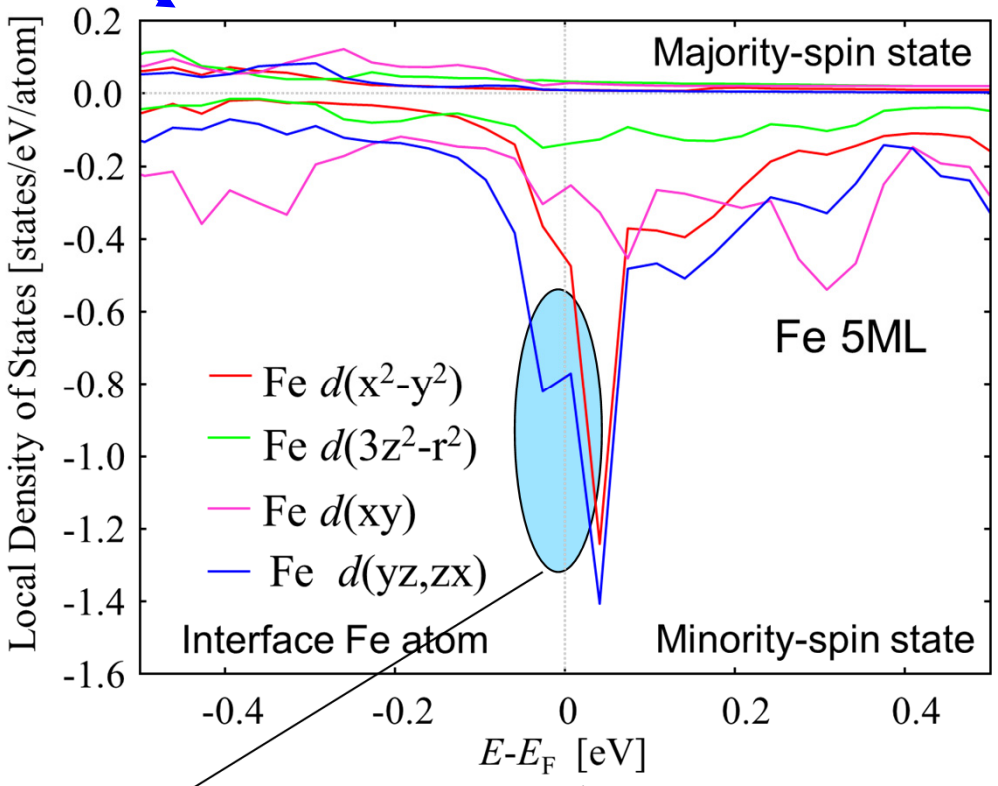

Large matrix element of $\langle d(x^2-y^2)|L^-|d(yz,zx)\rangle$

Increase damping with increasing EF

Second order perturbation of SOI

D. Wang, et al., PRB **47**, 14932 (1993).

$$E_{\mathrm{PMA}} \propto (\xi)^2 \sum_{o,u,k} \frac{\left|\langle o,k,\downarrow|L_z|u,k,\downarrow\rangle\right|^2 - \left|\langle o,k,\downarrow|L_x|u,k,\downarrow\rangle\right|^2}{\varepsilon^{\downarrow}_{u,k} - \varepsilon^{\downarrow}_{o,k}}$$

$$L_x = \tfrac{1}{2}\left(L^- + L^+\right)$$

The $\langle d(x^2\text{-}y^2)|L^-|d(yz)\rangle$ increase the damping, but decrease the PMA.⇒opposite EF dependence

Summary of the second topic

First principles study on voltage control of magnetic anisotropy (VCMA) and magnetic damping in Fe/MgO interface

- For Fe/MgO(001) surface, the magnetic damping increases with increasing the electron accumulation at interface (positive EF).

  (20% of damping constant α can be changed by EF=1[V/nm] for Fe/MgO(001))

- It is opposite to that of PMA (perpendicular magnetic anisotropy).

- The voltage dependence of magnetic damping of Fe/MgO(001) can be attributed to the spin conservation term.

Topics

0. Introduction on spintronics

1. First-Principles Study on magneto-crystalline anisotropy of Fe/MgO(001) and Fe/$MgAl_2O_4$(001)

K. Masuda and Y. Miura, PRB **98**, 224421 (2018).

2. First-Principles Study on magnetic damping of Fe/MgO(001)

Y. Miura, in preparation

3. First-Principles Study on magneto Seebeck Effect in magnetic tunnel junctions

K. Yamamoto, K. Masuda, K. Uchida, Y. Miura arXiv:1912.01207

Seebeck effect in MTJs

Seebeck coefficient: $S = \left(\frac{V}{\Delta T} \right)_{I=0}$

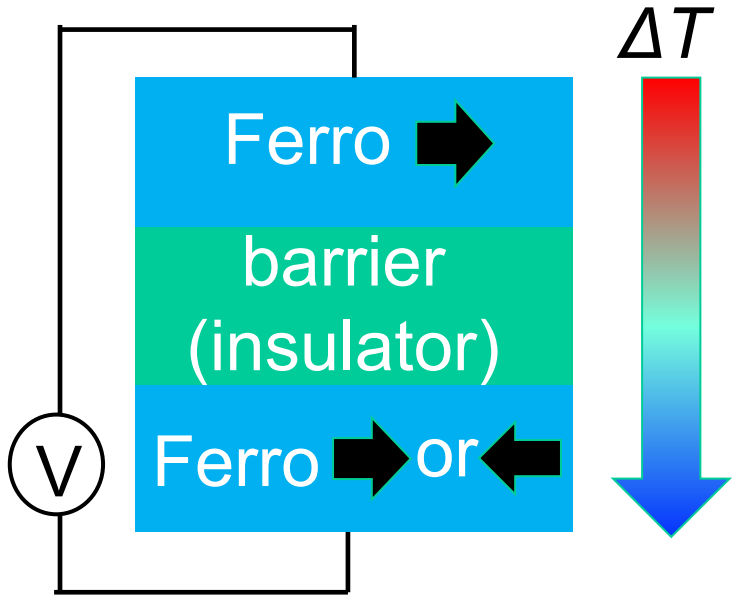

Spin caloritronics

Application

The change of Seebeck coefficients in parallel and anti-parallel magnetization
⇒Tunneling Magneto-Seebeck (TMS) effect

- Thermal readout of MRAM B. Geisler, P. Kratzer PRB. **92**, 144418 (2015).
- Thermal spin torque transfer X. Jia *et al.*, PRL. **107**, 176603 (2011).

Previous theoretical and experimental researches

- barrier: MgO, $MgAl_2O_4$
- electrode: Fe, FeCo, CoFeB, Heusler, etc…

First experiment: M. Walter *et al.*, Nat. Mater. **10**, 742 : Liebing *et al.*, PRL **107**, 177201 (2011).

Review: T. Kuschel *et al.*, J. Phys. D: Appl. Phys. **52**, 133001 (2019).

Enhancement of Seebeck effect

$$S = \left(\frac{V}{\Delta T}\right)_{I=0} = -\frac{L_{12}}{TL_{11}} = -\frac{\int \tau(E)(E-E_F)\left(-\frac{\mathrm{d}f}{\mathrm{d}E}\right)dE}{eT\int \tau(E)\left(-\frac{\mathrm{d}f}{\mathrm{d}E}\right)dE}$$

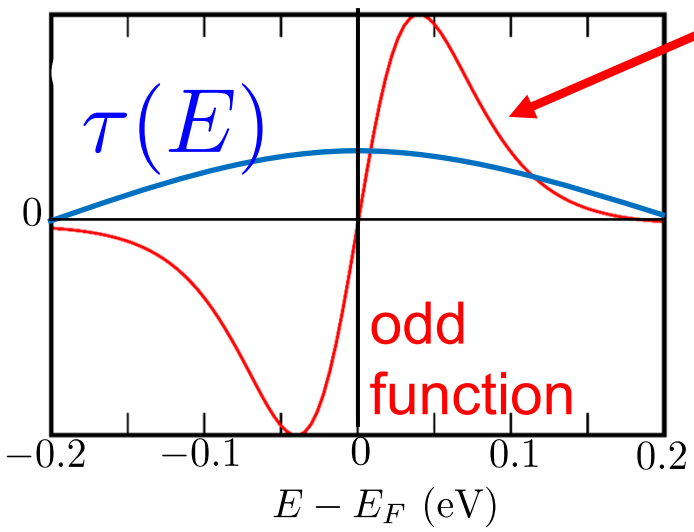

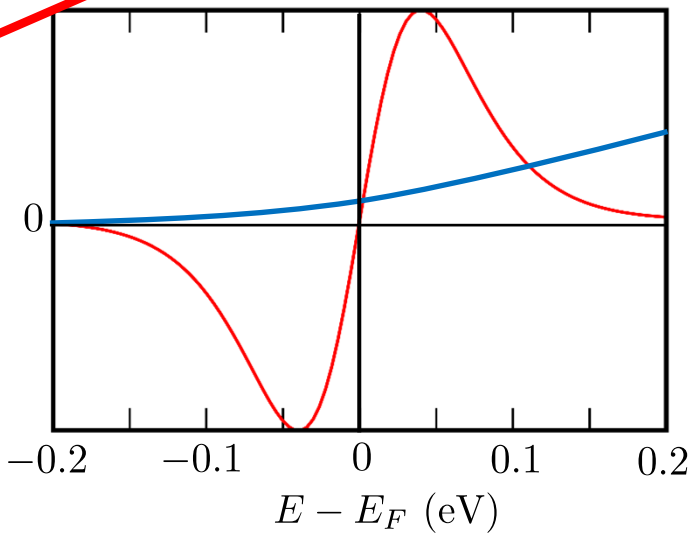

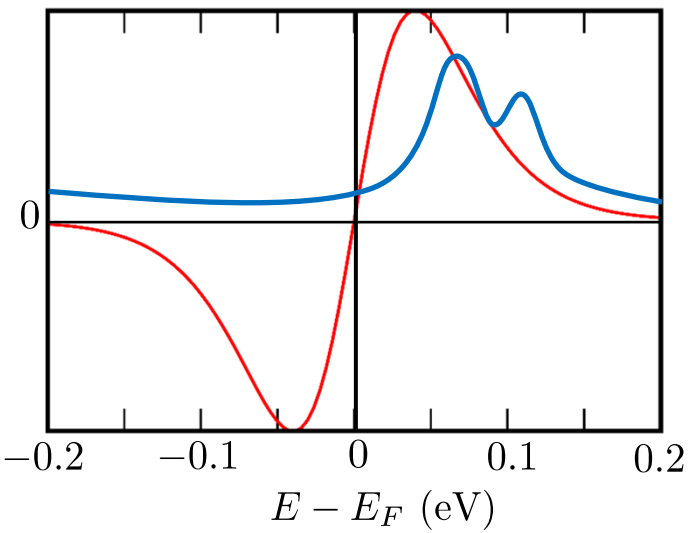

Symmetric $\tau(E)$ → $S = 0$

weak asymmetric $\tau(E)$ → small S

strong asymmetric $\tau(E)$ → large S

Interface resonant tunneling

Interface resonant tunneling

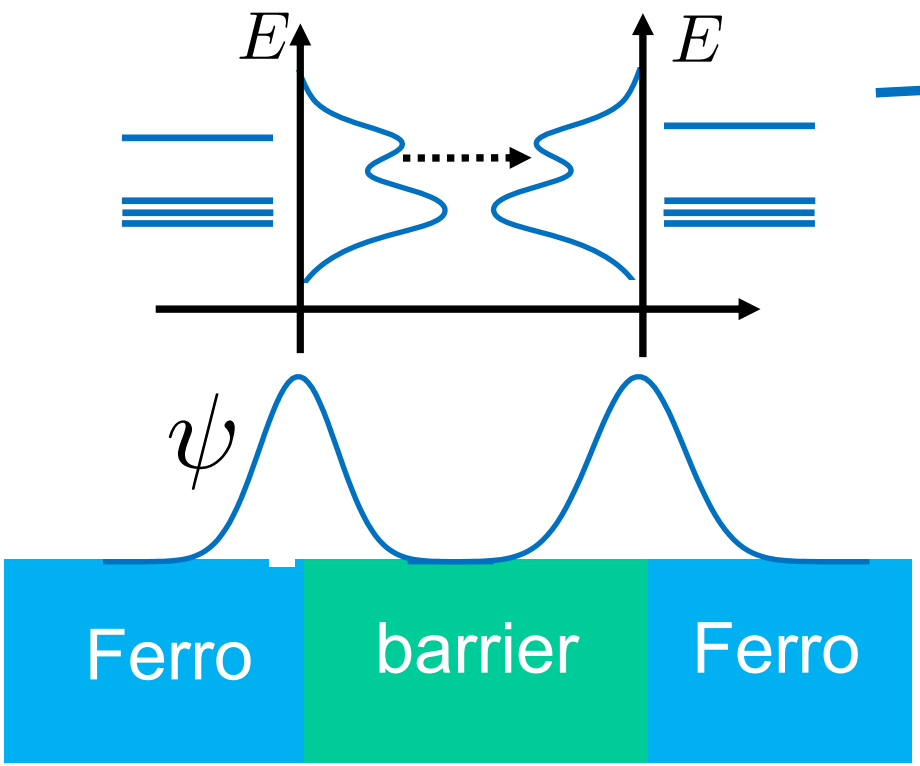

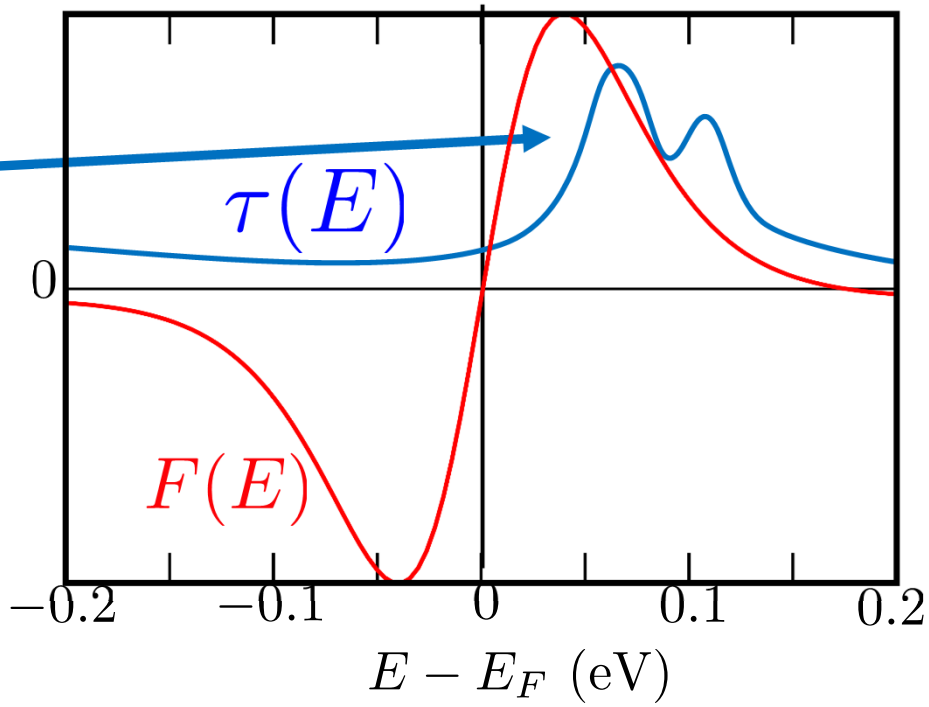

Fe/MgO/Fe MTJ is known to have interface resonant tunneling

W. H. Butler *et al.*, PRB **63**, 056614(2001).

J. Mathon, A. Umerski, PRB **63**, 220403 (2001).

Interface resonant tunneling

→ asymmetric peak

→ large Seebeck coefficient

Purpose of this work

To clarify the effects of structural parameters on the interface resonant tunneling and the Seebeck effects of MTJs.

Fe(7ML)/MgO(*n*ML)/Fe(7ML) MTJ in parallel magnetization

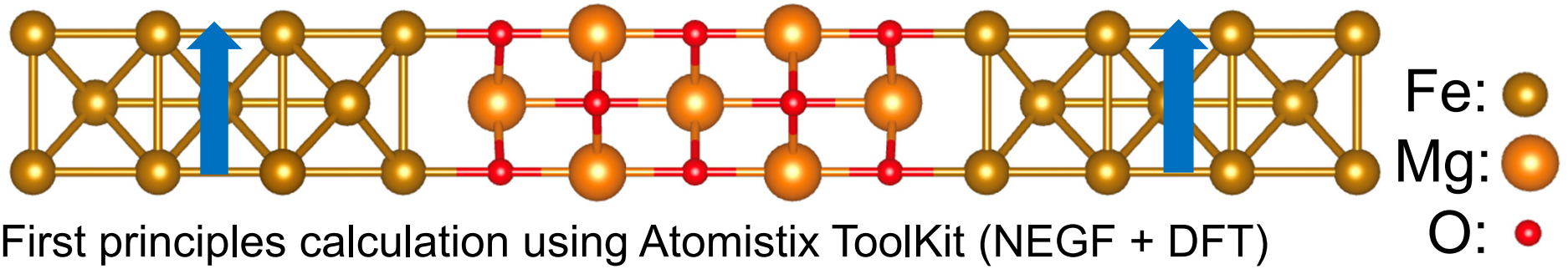

First principles calculation using Atomistix ToolKit (NEGF + DFT)
Atomic positions perpendicular to the plane are fully relaxed.

Changing structural parameters of MTJs

1: The MgO barrier thickness (3ML ~ 12ML)

2: In-plane lattice distortion

$$a = a_{\mathrm{Fe}} \fallingdotseq 2.87 \text{ Å}$$

Compressive in-plane lattice distortion

➡ Increase of perpendicular atomic distance

$$a = a_{\mathrm{MgO}}/\sqrt{2} \fallingdotseq 2.978 \text{ Å}$$

Extensive in-plane lattice distortion

➡ decrease of perpendicular atomic distance

Seebeck coefficient of Fe(7ML)/MgO(nML)/Fe(7ML)

For parallel magnetization @ 300 K

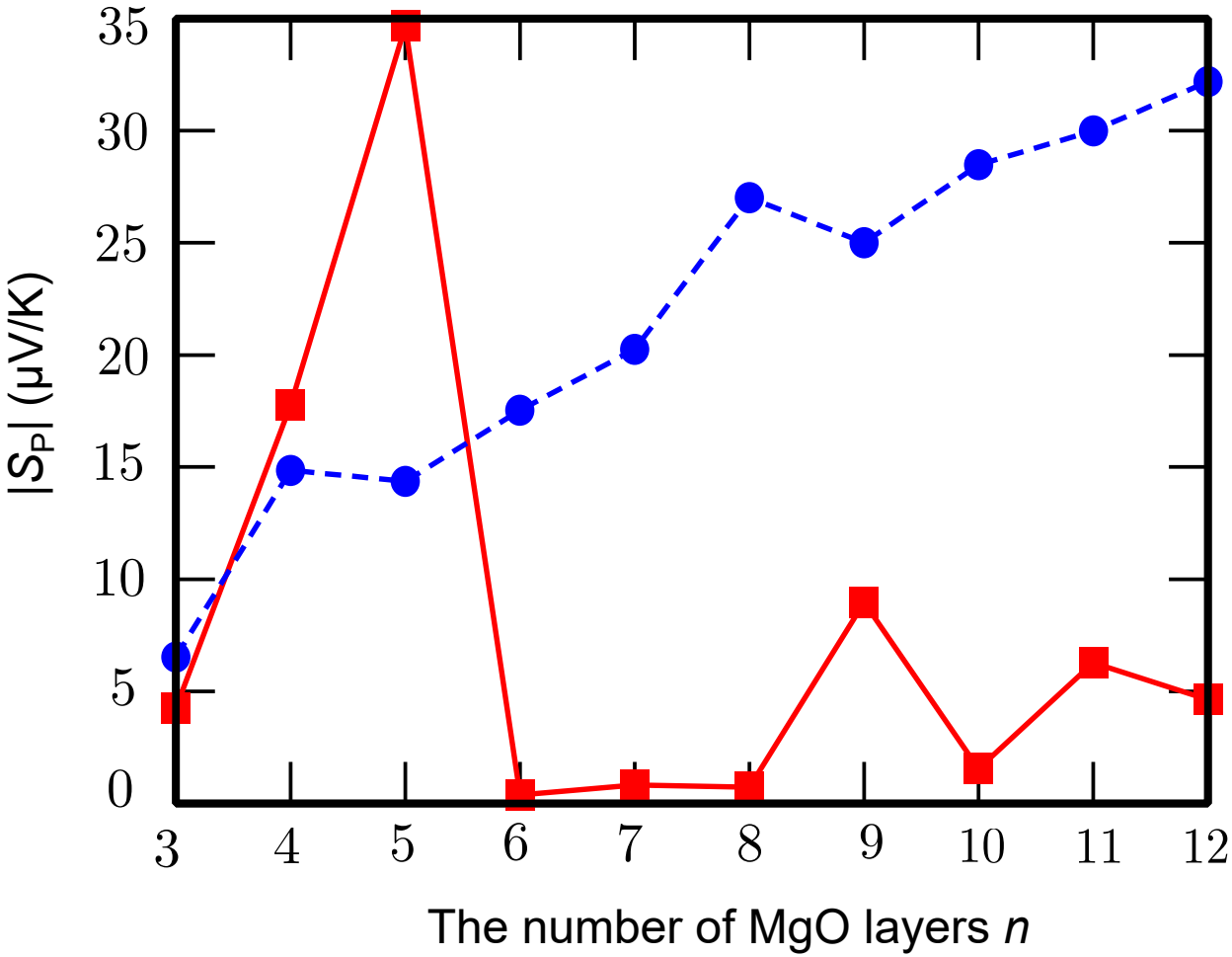

■ $a = a_{\mathrm{Fe}} \fallingdotseq 2.87$ Å

(compressive in-plane lattice distortion)

● $a = a_{\mathrm{MgO}}/\sqrt{2} \fallingdotseq 2.978$ Å

(extensive in-plane lattice distortion)

Behavior of the Seebeck effect is different between two in-plane lattice distortions.

Fe(7ML)/MgO(***n***ML)/Fe(7ML)
parallel magnetization configuration

Compressive in-plane lattice distortion

$a = a_{\mathrm{Fe}} \fallingdotseq 2.87$ Å

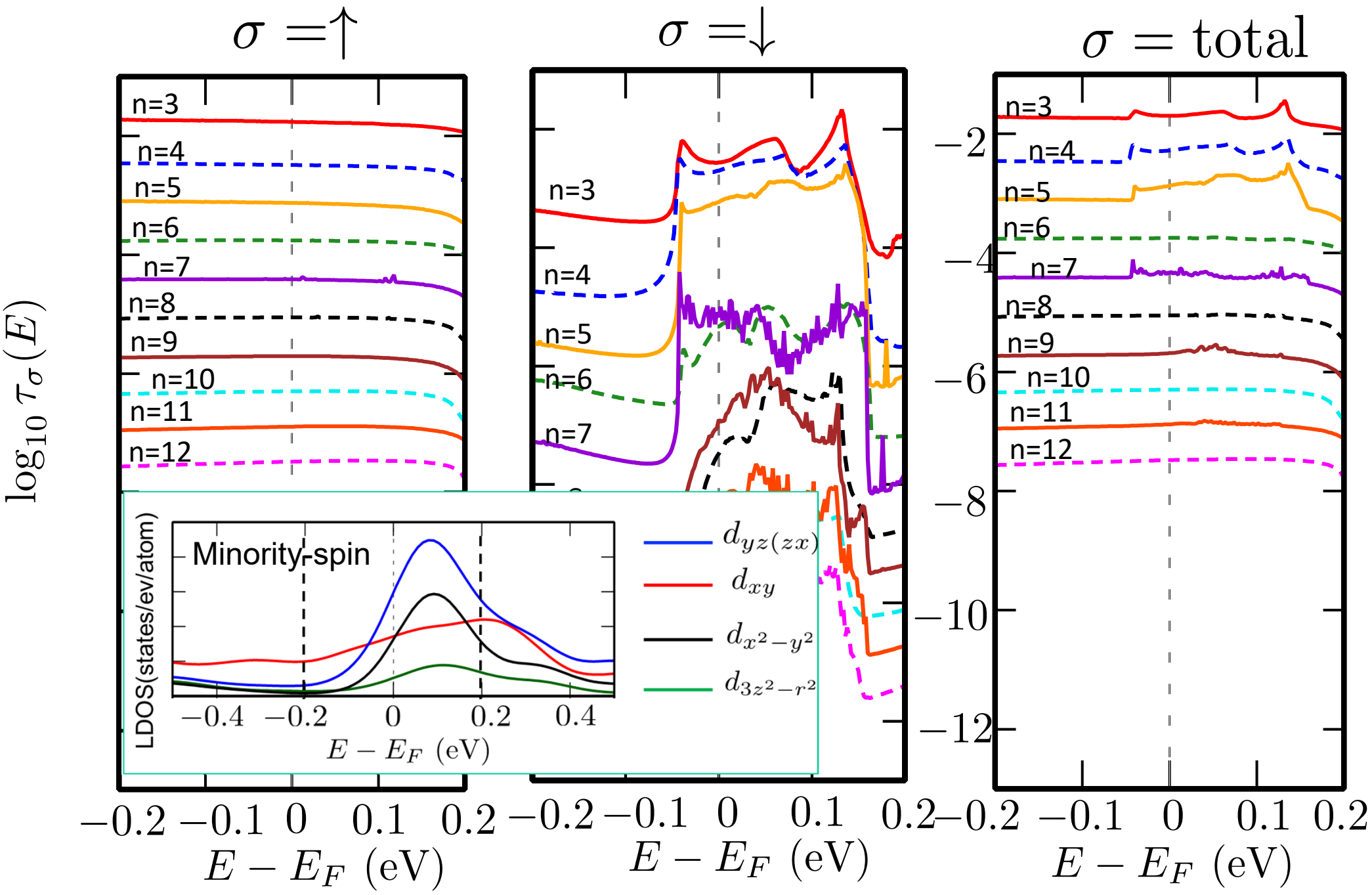

Fe(7ML)/MgO(**n**ML)/Fe(7ML)

parallel magnetization configuration

Extensive in-plane lattice distortion

$a = a_{\mathrm{MgO}}/\sqrt{2} \fallingdotseq 2.978$ Å

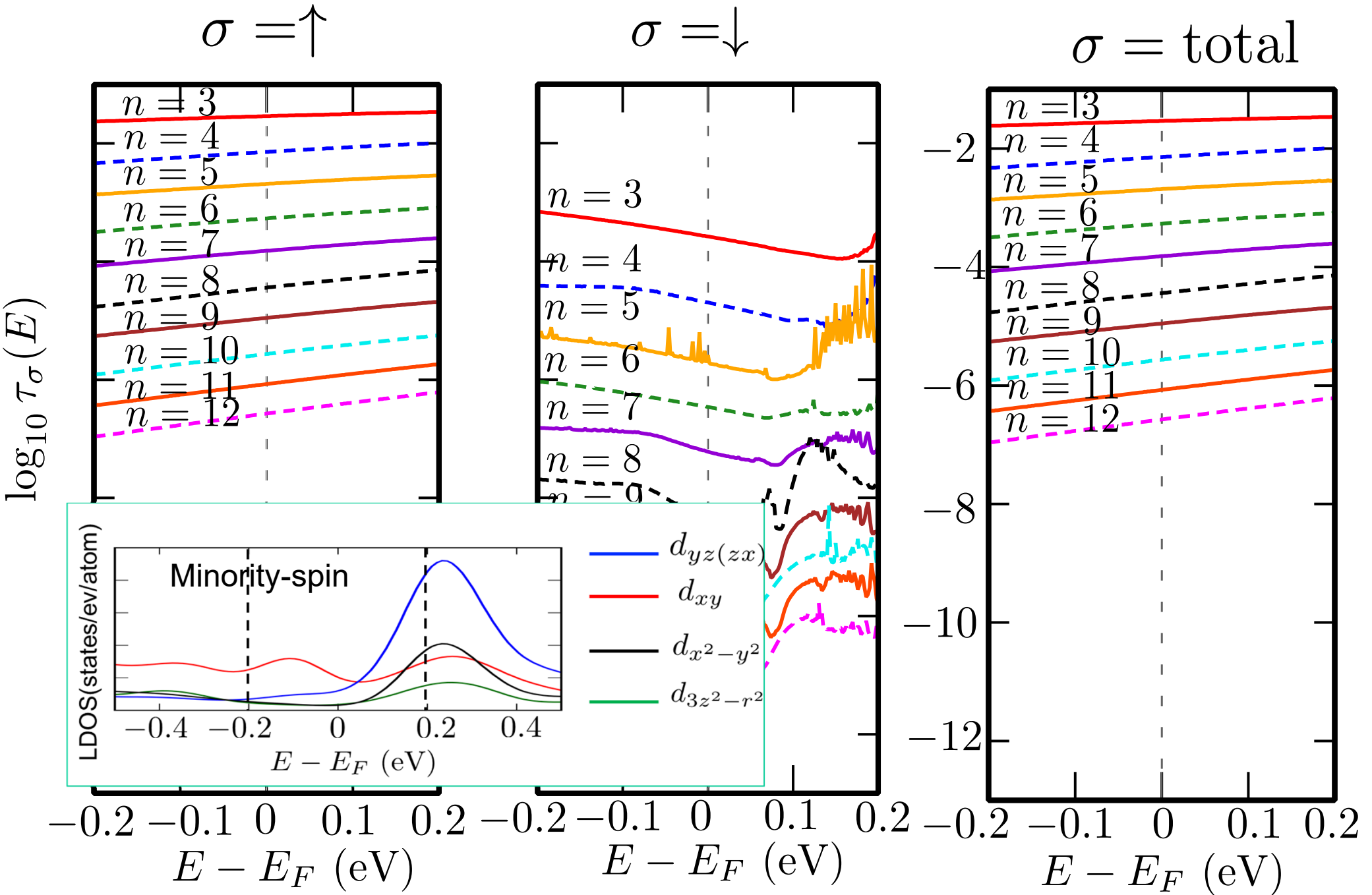

Why interface resonant states shift by in-plane distortion?

$a = a_{\mathrm{Fe}} \fallingdotseq 2.87$ Å

Compressive in-plane lattice distortion

$a = a_{\mathrm{MgO}}/\sqrt{2} \fallingdotseq 2.978$ Å

Extensive in-plane lattice distortion

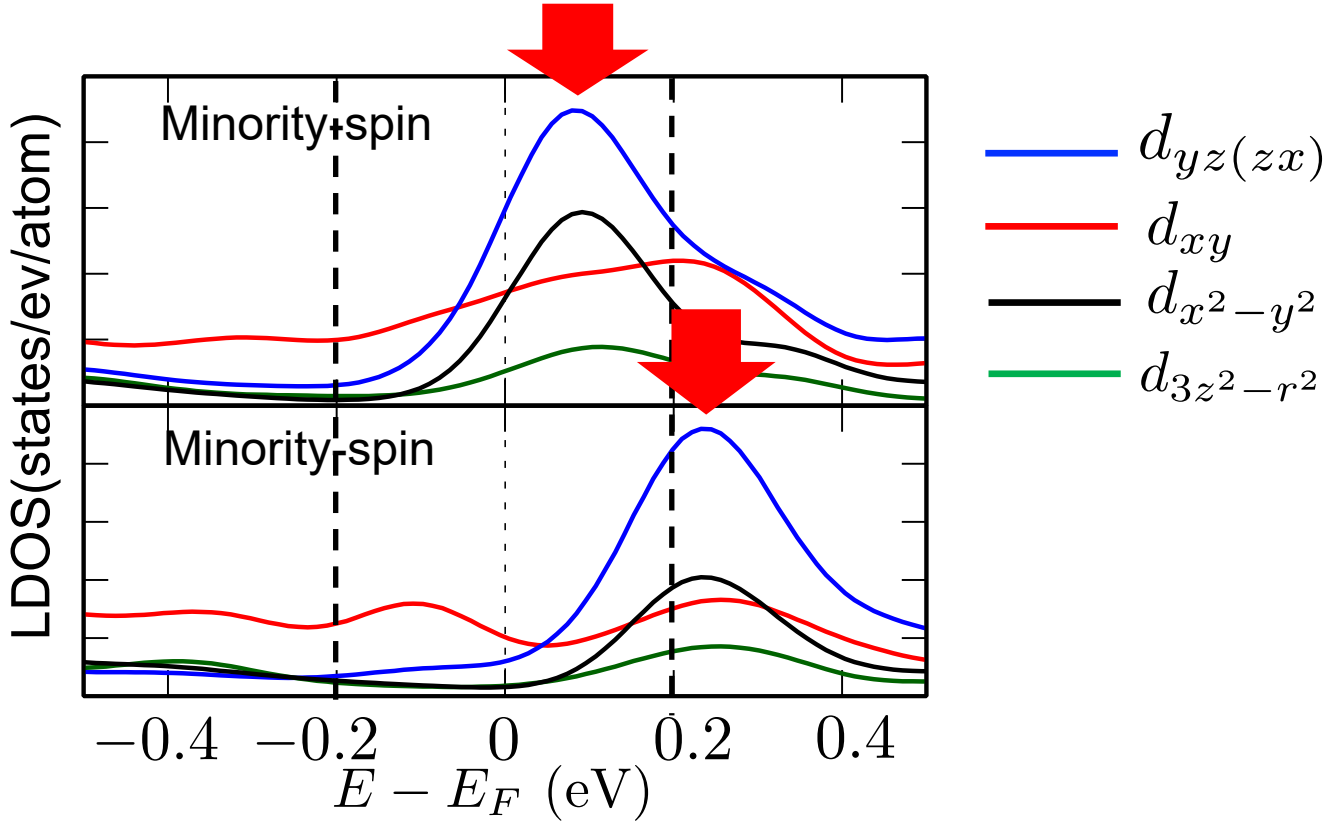

These interfacial states are mainly composed of antibonding states of interfacial Fe d(yz,zx).

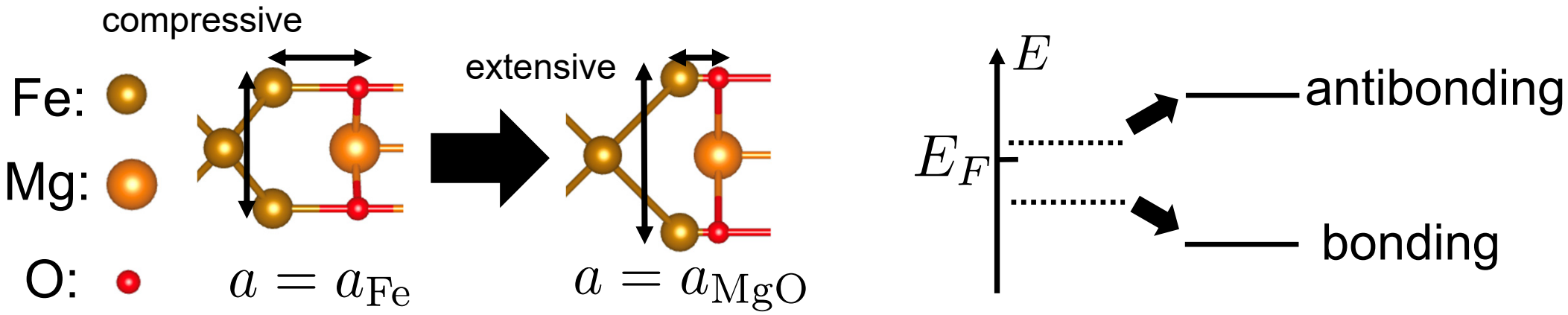

Power factor* (Conductance/A・Seebeck^2) of Fe(7ML)/MgO(nML)/Fe(7ML)

Characterized output electric power, $S^2 \cdot G/A$

For parallel magnetization @ 300 K

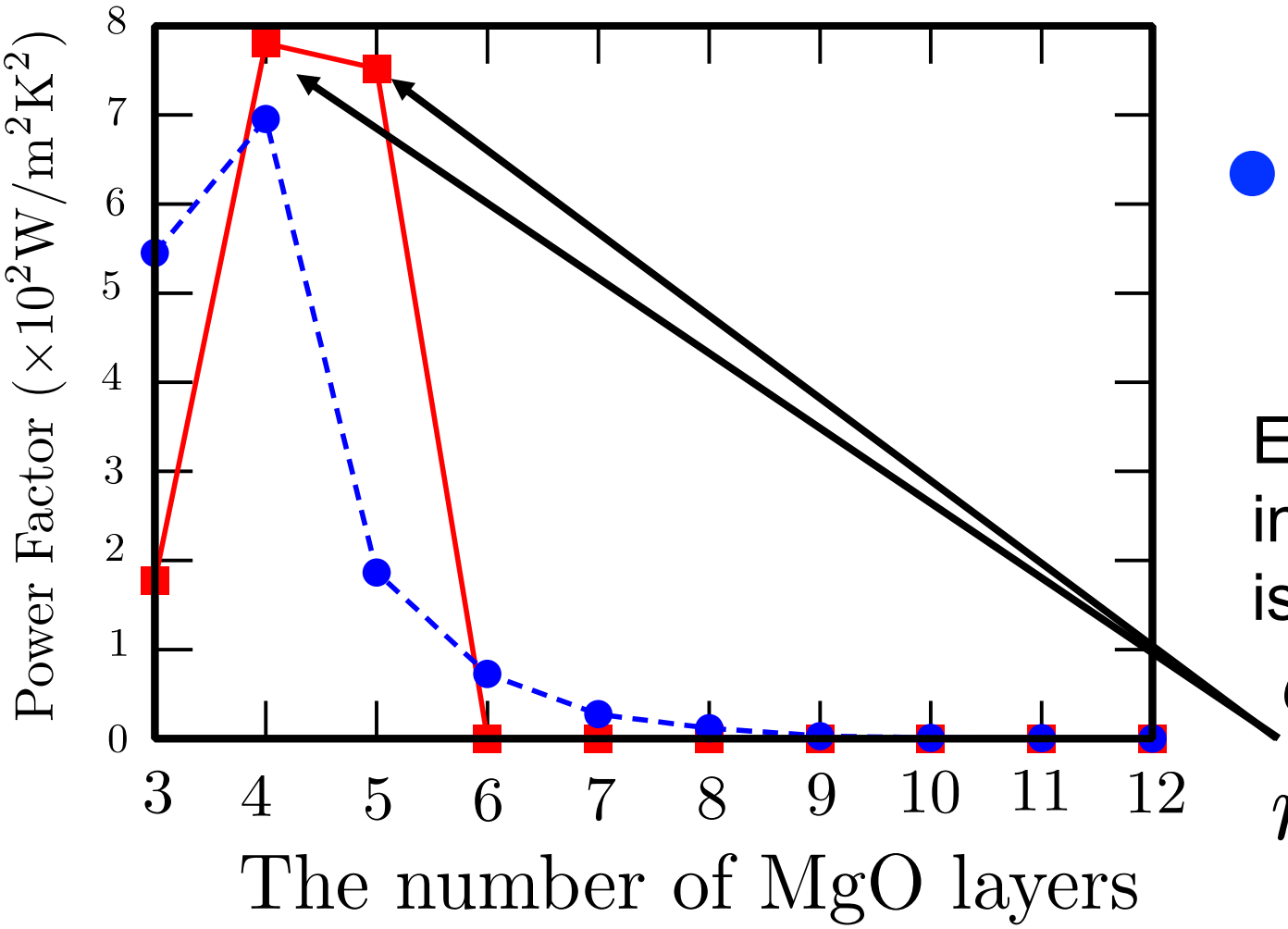

■ $a = a_{\mathrm{Fe}} \fallingdotseq 2.87$ Å

(compressive in-plane lattice distortion)

● $a = a_{\mathrm{MgO}}/\sqrt{2} \fallingdotseq 2.978$ Å

(extensive in-plane lattice distortion)

Effect of the interface resonance is large at:

$a = a_{\mathrm{Fe}}$

$n = 4, 5$

(1nm)

Summary of the Third topic

- Ab-initio calculation of the Seebeck coefficient in MTJ

- Interface resonant tunneling in Fe/MgO(nML)/Fe enhances the Seebeck coefficient with 1 nm MgO thickness (n= 4,5) and the compressive in-plane lattice distortion (a=a_{Fe})

- Control of MgO thickness and in-plane lattice distortion is significant to enhance the Seebeck coefficient and power factor

arXiv:1912.01207